

The Texas Medical Center Library

DigitalCommons@TMC

The University of Texas MD Anderson Cancer
Center UTHealth Graduate School of
Biomedical Sciences Dissertations and Theses
(Open Access)

The University of Texas MD Anderson Cancer
Center UTHealth Graduate School of
Biomedical Sciences

12-2012

MUTATIONS IN STAT3 ASSOCIATED WITH HUMAN HYPER IgE SYNDROME ENHANCE NF κ B AND MAPK-MEDIATED GENE EXPRESSION

Nathaniel Greeley

Follow this and additional works at: https://digitalcommons.library.tmc.edu/utgsbs_dissertations



Part of the [Biology Commons](#), and the [Immunology and Infectious Disease Commons](#)

Recommended Citation

Greeley, Nathaniel, "MUTATIONS IN STAT3 ASSOCIATED WITH HUMAN HYPER IgE SYNDROME ENHANCE NF κ B AND MAPK-MEDIATED GENE EXPRESSION" (2012). *The University of Texas MD Anderson Cancer Center UTHealth Graduate School of Biomedical Sciences Dissertations and Theses (Open Access)*. 305. https://digitalcommons.library.tmc.edu/utgsbs_dissertations/305

This Thesis (MS) is brought to you for free and open access by the The University of Texas MD Anderson Cancer Center UTHealth Graduate School of Biomedical Sciences at DigitalCommons@TMC. It has been accepted for inclusion in The University of Texas MD Anderson Cancer Center UTHealth Graduate School of Biomedical Sciences Dissertations and Theses (Open Access) by an authorized administrator of DigitalCommons@TMC. For more information, please contact digitalcommons@library.tmc.edu.

The
TMC LIBRARY
Health Sciences Resource Center

MUTATIONS IN STAT3 ASSOCIATED WITH HUMAN HYPER IgE SYNDROME
ENHANCE NF κ B AND MAPK-MEDIATED GENE EXPRESSION

A
THESIS

Presented to the Faculty of
The University of Texas
Health Science Center at Houston
and
The University of Texas
MD Anderson Cancer Center
Graduate School of Biomedical Sciences
In Partial Fulfillment
of the Requirements
for the Degree of
MASTER OF SCIENCE

by
Nathaniel Robert Greeley, B.A.
Houston, Texas
December, 2012

Dedication

To my wife, Samantha; my parents, Laura and Dave; and my friends and co-workers who supported me throughout.

Abstract

Hyper IgE syndrome (HIES) is a multisystem disorder resulting in bone and immune system abnormalities. It is associated with mutations in *STAT3*, which disrupt protein domains responsible for transcriptional function. Patients with HIES display osteoporosis and enhanced inflammatory cytokine production similar to hematopoietic *Stat3*-deficient mice. Since osteoclast and inflammatory cytokine genes are NFkB targets, these observations indicate a possible deregulation of NFkB signaling in both mice and humans with STAT3-deficiency. Here, we sought to examine the role of STAT3 in the regulation of NFkB-mediated gene expression through analysis of three HIES STAT3 point mutations in both hematopoietic and non-hematopoietic cells. We found that IL-6-induced tyrosine phosphorylation of STAT3 was partially or completely abrogated by HIES mutations in the transactivation domain (V713L) or SH2 domain (V637M), respectively, in both hematopoietic and non-hematopoietic cells. By contrast, IL-6-induced tyrosine phosphorylation of an HIES mutant in the STAT3 DNA-binding domain (R382W) was intact. The R382W and V713L mutants significantly reduced IL-6-dependent STAT3 transcriptional activity in reporter gene assays. Moreover, the R382W and V637M mutants significantly diminished IL-6-responsive expression of the endogenous STAT3 target gene, *Socs3*, as assessed by quantitative real-time PCR (qPCR) in the RAW macrophage cell line. These observations indicate the HIES mutants dominantly suppress the transcriptional activity of wild type STAT3, albeit to varying degrees. All three HIES mutants enhanced LPS-induced expression of the NFkB target genes *IL6* (IL-6), *Cxcl10* (IP-10), and *Tnf* (TNF α) in RAW cells, as indicated by qPCR. Furthermore, overexpression of wild type STAT3 in *Stat3*-deficient murine embryonic fibroblasts significantly reduced LPS-stimulated expression of *IL6*, *Cxcl10*, and *IL12p35*. In addition, in a

primary murine osteoclast differentiation assay, a STAT3-specific SH2 domain inhibitor led to significantly increased levels of osteoclast-specific gene expression. These results suggest that STAT3 serves as a negative regulator of NF κ B-mediated gene expression, and furthermore imply that STAT3 mutations associated with HIES contribute to the osteopenia and inflammation observed in HIES patients.

Table of Contents

Approval Signatures	i
Title Page	ii
Dedication	iii
Abstract	iv
Table of Contents	vi
List of Illustrations	viii
List of Tables	x
<u>Introduction</u>	1
Hematopoiesis	1
Osteoclastogenesis	1
NFκB-mediated inflammation	7
JAK/STAT pathway	13
STAT3	16
STAT3 and inflammation	20
STAT3 and cancer	21
Hyper IgE syndrome	22
Project Goal	25
<u>Materials and Methods</u>	25
Cell lines, Culture Conditions, and Cytokine treatments	25
STAT3 mutant generation	26
Production of retrovirus	27
STAT3 SH2 domain inhibitor	27
Preparation of whole cell lysates, gels, and immunoblots	28
Quantitative Real-time PCR	29

Oligonucleotide sequences	29
Transient Transfection for STAT3 overexpression	29
FLAG-immunoprecipitation and immunoblotting	31
Transfection of STAT3-deficient MEFs	31
Luciferase assays	32
<u>Results</u>	32
Generation of the STAT3 mutant constructs	32
Effect of HIES mutants upon endogenous STAT3 phosph.	38
Activation of STAT3 HIES mutants	41
Transcriptional activity of STAT3 HIES mutants	49
Dominant negative effects of STAT3 HIES mutants	52
Effect of STAT3 function on osteoclast gene expression	58
Effect of HIES mutations on inflammatory gene expression	59
LPS-induced inflammatory gene expression in MEFs	67
HIES mutants' effect on inflammatory gene expression in MEFs	70
HIES mutants' effect on LPS-induced MAPK signaling	73
<u>Discussion</u>	76
<u>References</u>	91
<u>Vita</u>	109

List of Illustrations

1a. Hematopoiesis	3
1b. Osteoclastogenesis	6
2. RANKL signaling pathway	9
3. TLR4 signaling pathway	12
4. JAK/STAT pathway	15
5. STAT3 protein structure	18
6. STAT3 truncation and HIES mutants	35
7. STAT3 HIES mutants in 293T cells	37
8. STAT3 mutants stably expressed in RAW cells	40
9. Total STAT3 Tyrosine phosphorylation in RAW cells	43
10. STAT3 HIES mutants in STAT3-deficient MEFs	46
11. Tyrosine phosphorylation of STAT3 HIES mutants in STAT3-deficient MEFs	48
12. <i>Socs3</i> expression in HIES mutant-expressing STAT3-deficient MEFs	51
13. HIES mutant Dominant negative activity in a luciferase assay	54
14. <i>Socs3</i> expressing HIES mutant-expressing RAW cells	57
15. Effect of the STAT3 inhibitor on tyrosine phosphorylation	61
16. RANKL induced osteoclast gene expression after STAT3 inhibition	63
17. HIES mutant effect on inflammatory gene expression in RAW cells	66
18. WT STAT3 effect on inflammatory gene expression in MEFs	69
19. HIES mutant effect on inflammatory gene expression In MEFs	72
20. HIES mutant effect on MAPK activation in RAW cells	75

21. WT STAT3/NF κ B interplay	88
22. HIES/ NF κ B interplay	90

List of Tables

1. Phenotype of STAT3-deficient mice and HIES patients	23
2. Sequence of qPCR oligonucleotides	30

Introduction

Hematopoiesis:

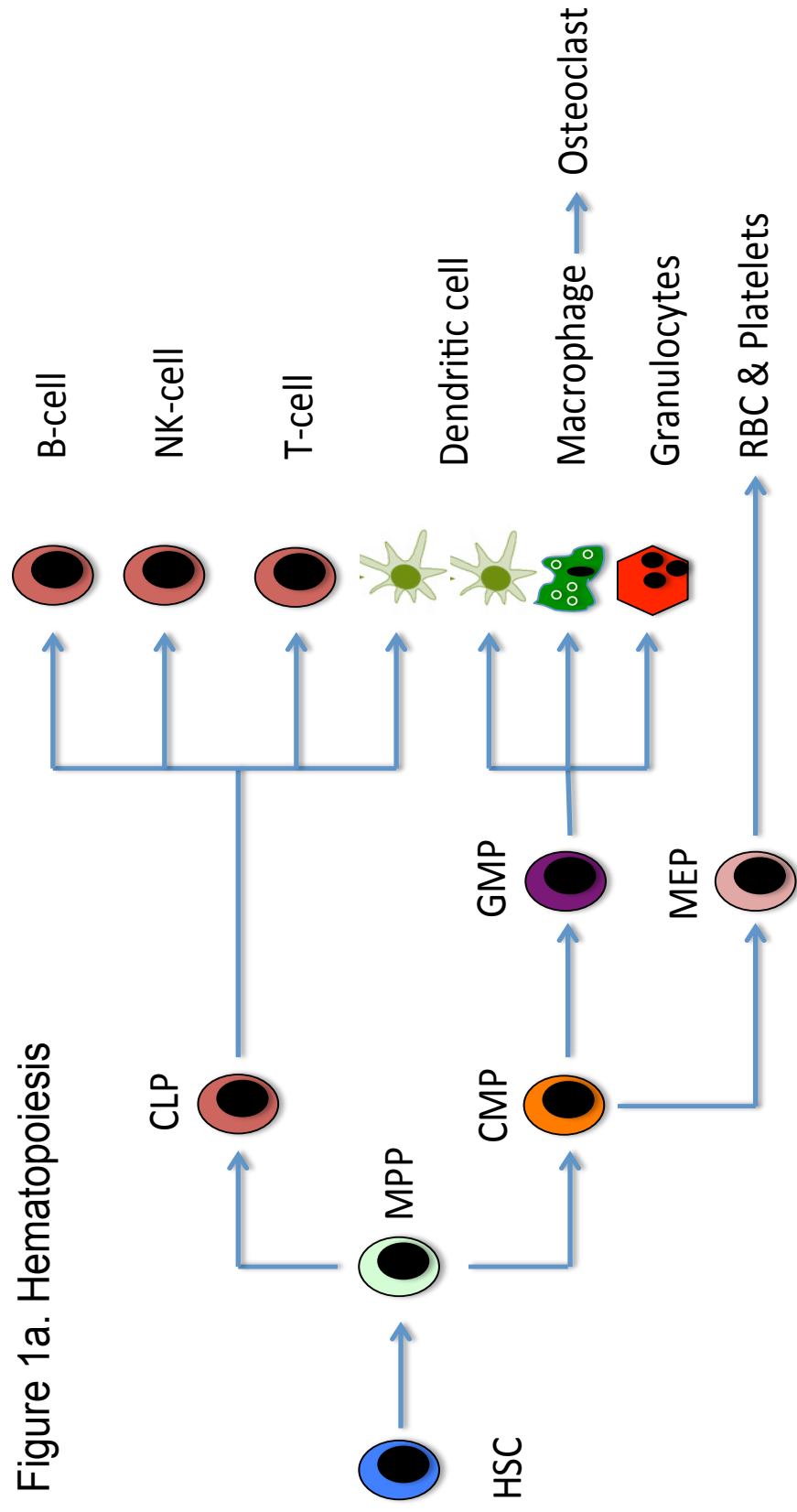
The cellular components of the immune system are generated through the process of hematopoiesis or blood formation. This begins with the differentiation of pluripotent hematopoietic stem cells (HSCs) in the bone marrow to a multipotent progenitor (MPP) and eventually to the development of the various effector subsets of both innate and adaptive immunity (Figure 1a) [1]. The cells of the adaptive immune response, namely T- and B- lymphocytes, differentiate from the common lymphoid progenitor (CLP), whereas the generation of innate immune cells occurs primarily through a process known as myelopoiesis, beginning with the common myeloid progenitor (CMP). These cells include the granulocytes (neutrophils, basophils, and eosinophils), dendritic cells, and macrophages. They act to protect the body from infection through secretion of various inflammatory cytokines along with physically interacting with the pathogens to remove them from the system. Macrophages are a prime example of this. However, given the right cytokine milieu, macrophages can also continue to differentiate further into cells known as osteoclasts in a process termed osteoclastogenesis.

Osteoclastogenesis:

The bone microenvironment is a highly dynamic system under the control of two main cell types: bone-producing osteoblasts and bone-resorbing osteoclasts. In normal individuals, there exists a unique balance between the functions of these two cell types to maintain a consistent bone density. However in individuals where one of these cell types is either over- or under-reactive, the pathologies of osteopetrosis

Figure 1a. Schematic representation of hematopoiesis, the process by which the cells of innate and adaptive immunity are formed.

Figure 1a. Hematopoiesis

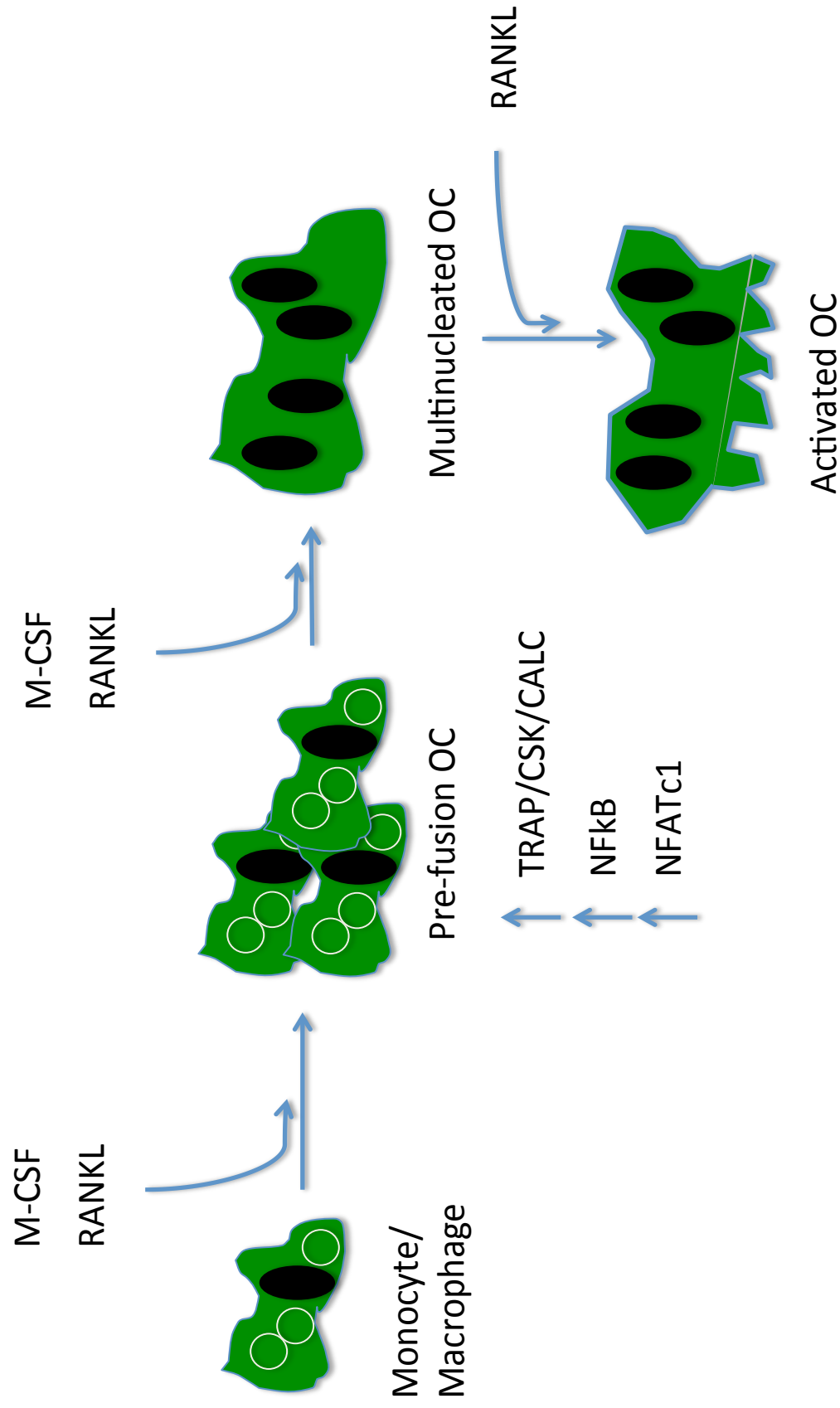


(bone hardening) or osteoporosis (reduced bone density) arise. The osteoclastogenesis pathway, beginning with the hematopoietic stem cells through the monocyte/macrophage lineage and eventually terminating in the production of bone-resorbing osteoclasts, is under the control of multiple cytokine as well as transcription factor signals (Fig. 1b). The Receptor-activator of NF κ B (RANK) pathway is essential for osteoclastogenesis and disruption of this pathway leads to severe osteopetrosis [2][3][4]. *In vitro*, osteoclasts are generated from bone marrow macrophages after addition of the soluble ligand for RANK, RANK ligand (RANKL), for 3-5 days and develop generally from fusion of multiple macrophages to form the multinucleated osteoclasts, which possess the ability to resorb bone [5][6].

RANK has been identified as a member of the tumor necrosis factor receptor (TNFR) super family [7]. In a ligand-dependent manner [8], after binding of RANKL, the receptor trimerizes, inducing recruitment of members of the TNFR-associated factor (TRAF) family, primarily TRAF6 although TRAFs 1, 2, 3, and 5 have been shown to bind RANK *in vitro* [9]. TRAF6 is an E3-ubiquitin ligase, and functions as such in concert with an E2-ubiquitin conjugating complex of Ubc13 and Uev1A [10]. Uev1A, an E1-ubiquitin ligase, activates the ubiquitin monomers and then subsequently transfers them transiently to Ubc13, an E1/E2-ubiquitin conjugating enzyme. Ubc13 then transfers the activated ubiquitin to TRAF6, which ligates it to its

Figure 1b. Schematic representation of osteoclastogenesis, the process by which cells of the monocyte/macrophage lineage differentiate to form the bone resorbing osteoclasts which are necessary for bone development and homeostasis.

Figure 1b. Osteoclastogenesis



target proteins [11]. Upon RANK activation, the TRAF6/Ubc13/Uev1A complex is recruited to a specific motif, on the cytoplasmic tail of RANK, which it binds with high affinity [12]. Through auto-ubiquitination of TRAF6 on a lysine residue at position 63, known as K63-linked polyubiquitination, Tak1-binding protein 2 (TAB2) can bind TRAF6. TAB2 then acts as a scaffold to allow binding of the TGF β -activating kinase 1 (TAK1)/Tak1-binding protein 1 (TAB1) complex [13]. This association of TAK1/TAB1 with TRAF6 allows TRAF6 to ubiquitinate TAK1, thus activating it [14]. This complex goes on to activate both the MAPK and the NF κ B signaling pathways via phosphorylation cascades resulting in activation of AP-1 and Nuclear Factor-kappa B (NF κ B), respectively (Figure 2).

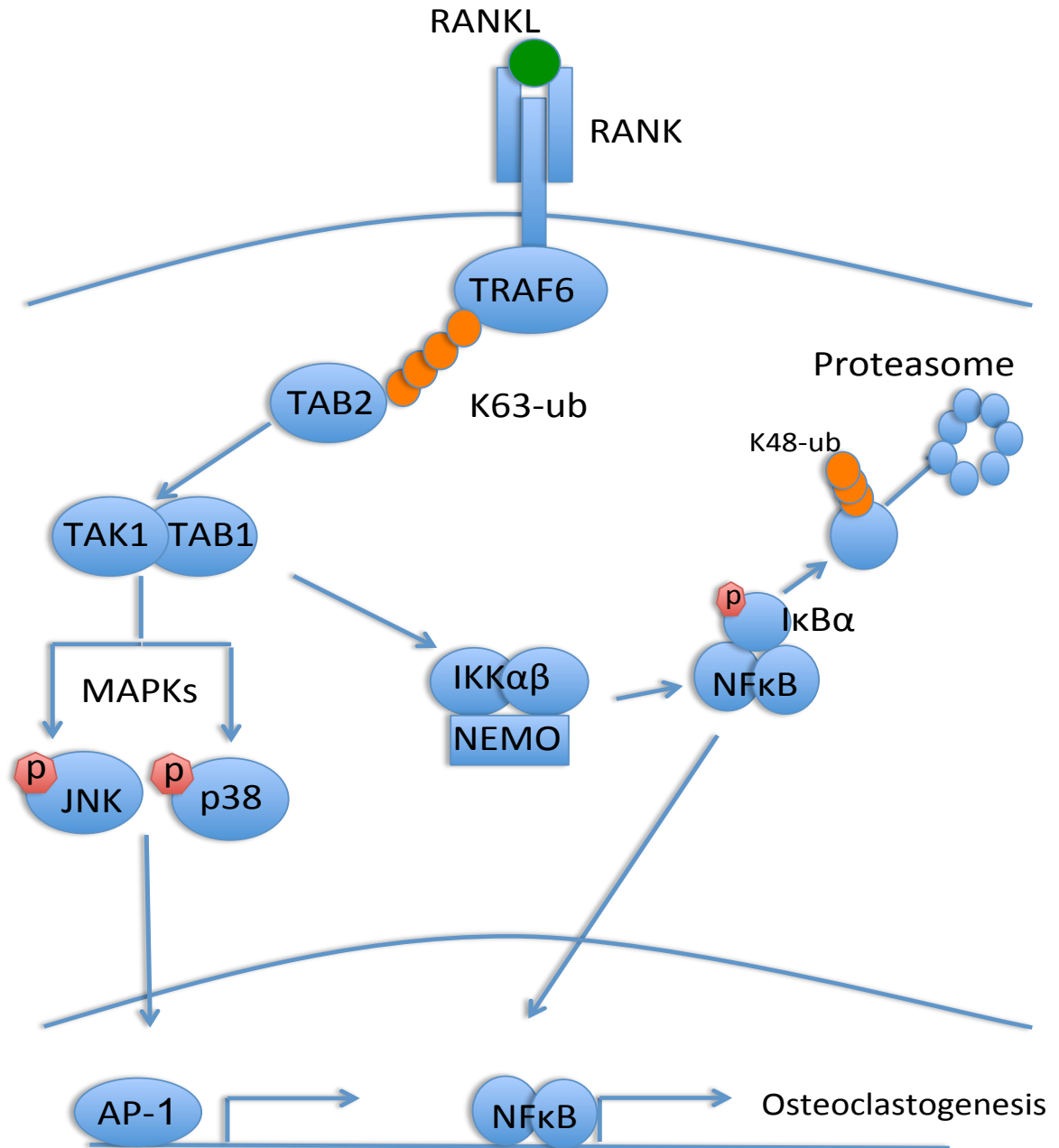
Activation of the RANK signaling pathways in osteoclast precursors eventually leads to the terminal differentiation of multinucleated osteoclasts capable of resorbing bone matrix. These osteoclasts have multiple phenotypic markers that serve as identifiers of the stage of osteoclast differentiation. As the osteoclast precursors begin to fuse, they up-regulate Tartrate-resistant acid phosphatase (TRAP) and Calcitonin receptor (CALC) on the cell surface [15]. Cathepsin K (CSK), a cysteine protease, is also up-regulated at this point and primarily functions in the resorptive process [16].

NF κ B-mediated inflammation:

While the TRAP, CALC and CSK osteoclast-specific markers have not been determined to be direct targets of NF κ B, it is clear that NF κ B is an important modulator of osteoclast differentiation [17][18]. NF κ B also functions in the innate immune system. One of its main roles is in production of pro-inflammatory mediators [19][20][21] via pathways that have been activated by pathogens recognized via a set of innate immune receptors known as Toll-like receptors (TLRs), including TLR4

Figure 2. Schematic representation of RANKL signaling. After RANKL binding its cognate receptor, TRAF6 becomes ubiquitinated, activating it and allowing it to activate downstream signaling resulting in MAPK and NFkB activation. This activation leads to the transcription of osteoclast specific genes and the differentiation of macrophages into bone-resorbing osteoclasts.

Figure 2. RANKL
Signaling pathway



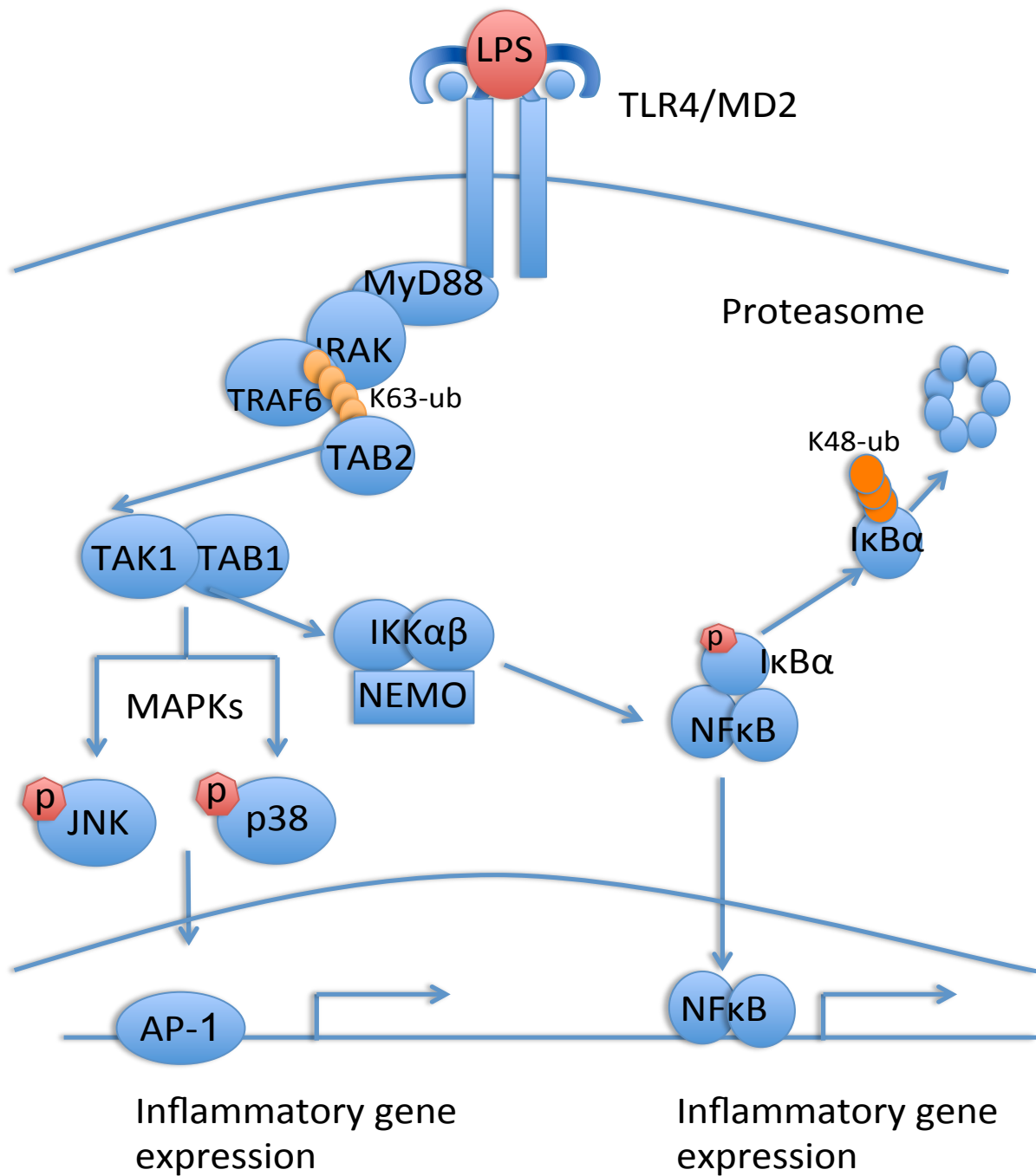
[22][23][24]. This inflammatory response is especially important for macrophages, as they are a primary effector of the innate immune system and one of the first defenses against infection [25].

Inflammatory signaling in macrophages occurs through various receptors both on the cell surface and in the cytosol. Macrophages highly express a variety of TLR, which recognize conserved pathogen-associated molecular patterns (PAMPs). These PAMPs are conserved motifs commonly found on different types of pathogens, including bacteria, fungi, and viruses. For example, TLR2 recognizes peptidoglycan, TLR7 recognizes single-stranded RNA, and TLR4 recognizes lipopolysaccharide (LPS) [22]. The effector products of each of the TLRs vary. Activation of TLR4, for example, induces activation of the NFkB and MAPK signaling cascades resulting in the production of a variety of inflammatory gene products [23][24][26].

Binding of LPS to TLR4 results in the dimerization of the receptors, and binding of the intracellular adaptor proteins TIR-domain-containing adapter-inducing interferon- β (TRIF) or myeloid differentiation primary response gene (MyD88) [27]. This elicits the binding and activation of IL1-receptor associated kinases 1, 2, and 4 (IRAK1/2/4) [28][29]. These adaptor molecules then recruit the E3-ubiquitin ligase TRAF6, similar to the RANK pathway. Polyubiquitinated TRAF6 then activates the NFkB and MAPK pathways as discussed previously, leading to expression of inflammatory cytokines including but not limited to tumor necrosis factor alpha (TNF α), Interleukin-6 (IL-6), IL-12, Interferon-gamma induced protein 10 (IP-10; Cxcl10), and IL1- β (Figure 3) [30][31][32][33]. Interestingly, LPS has also been shown to induce osteoclastogenesis from bone marrow precursors as one might expect from the similarity of the TLR4 and RANK signaling pathways [34][35].

Figure 3. Schematic representation of LPS-induced TLR4 signaling. After LPS binds, the receptor dimerizes and recruits the scaffold protein MyD88 resulting in the activation of IRAK and TRAF6. TRAF6 then activates downstream signaling events leading to NFκB and MAPK activation and the transcription of inflammatory genes such as IL-6, IP-10, IL-12, and TNFα.

Figure 3. TLR4 signaling pathway



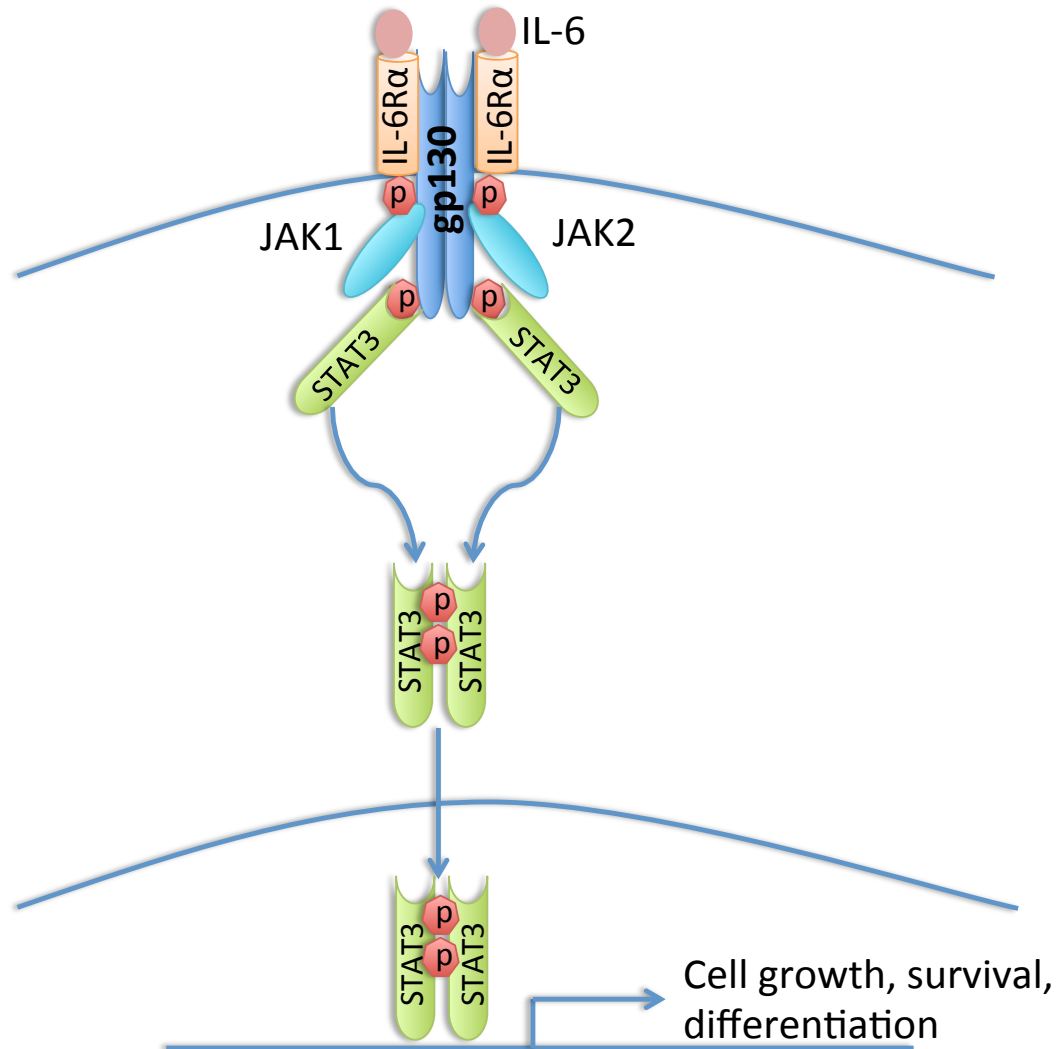
Another pathway highly important in myeloid cell development, function and inflammation is the JAK-STAT pathway [36-38]. Binding of a cytokine ligand to its cognate trans-membrane receptor primarily activates this pathway. The signal-transducer and activator of transcription (STAT) proteins have been shown to be important for myeloid cell development, homeostasis and function including inflammatory gene expression as discussed below [39-43].

The JAK/STAT pathway:

The STAT family of proteins consists of 7 members: STAT1, 2, 3, 5a, 5b, and 6 [44]. STATs can form homo- or hetero-dimers in the cytoplasm upon specific stimulation of growth factor or cytokine receptors on the cell surface. Once activated, the STATs function as transcription factors to regulate cell growth, differentiation, survival, and function [45]. Figure 4 depicts a more detailed look at how the cytokines transduce a STAT-dependent signal to the nucleus to stimulate gene transcription. After binding of the cytokine or growth factor ligand to the receptor, the monomers dimerize bringing the receptor-associated kinases on the cytoplasmic tails together [46][47]. This allows cross-phosphorylation of the kinases as well as the receptor cytoplasmic tails at specific tyrosine residues [47]. These phosphorylated residues create docking sites for the STAT proteins to bind via their Src-Homology 2 (SH2) domains [48]. The receptor-associated kinases then phosphorylate the STAT proteins on a specific tyrosine residue (Y705 for STAT3), allowing the STAT monomers to associate into dimers via SH2-phosphotyrosine-interactions [49][44]. These activated STAT dimers now translocate to the nucleus where they can function as transcription factors. This pathway has been termed the canonical pathway of STAT signaling [50].

Figure 4. Schematic representation of canonical STAT3 signaling. IL-6 binds IL-6R α , either soluble or membrane bound depending on the cell type. This complex binds the transmembrane signaling component, gp130. Dimerization of this receptor leads to cross-phosphorylation allowing the binding of JAK1/2. These kinases further tyrosine phosphorylate the receptor allowing STAT3 monomers to bind via their SH2 domain. JAK then phosphorylate STAT3 on tyrosine 705 allowing dimerization, nuclear translocation and transcription of STAT3 target genes like SOCS3.

Figure 4. Canonical JAK/STAT pathway



As was stated earlier, STATs function broadly in immune cell function, differentiation, and maintenance. The physiological role of each STAT family member has been widely studied through the use of both complete and conditional knockout mice [51]. While each is important in its own right, STAT3 has been the only STAT to show early embryonic lethality [52] which indicates its importance for cell growth, differentiation, and function early in the developmental process [53].

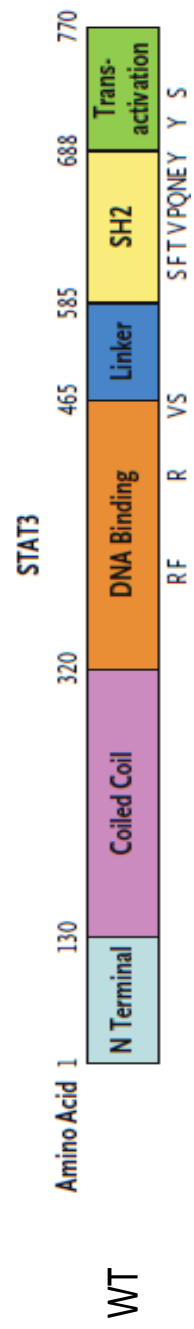
STAT3:

STAT3 has a structure like other STAT proteins (Figure 5). It contains an N-terminal region, followed by a coiled-coiled domain, and a DNA-binding domain [54][53]. The C-terminal region contains the SH2-domain and finally a transactivation domain (TAD) [53]. The important tyrosine residue is located in the SH2 domain adjacent to the TAD. A serine residue that also undergoes phosphorylation most likely via serine/threonine kinases is located in the TAD at position 727. Phosphorylation at this serine residue has been shown to enhance STAT3 mediated transcription [55] but is unnecessary for STAT3 DNA binding [56].

Signaling via STAT3 can occur similarly to other STAT proteins, via the canonical pathway (Figure 4). In the IL-6 response, STAT3 activation involves both the IL-6-receptor alpha chain (IL-6R α), which binds IL-6, followed by the binding of IL-6/IL-6R α to the signaling subunit, gp130 [57]. Additional cytokines that activate STAT3 via gp130 include: IL-10, IL-11, IL-21, IL-23, Leukemia Inhibitory Factor (LIF), and Oncostatin M (OSM). Granulocyte-colony stimulation factor (G-CSF) and Interferon-alpha/beta (IFN- α/β) also activate STAT3 although not through gp130-mediated signaling [58][59][60].

Figure 5. Schematic structure of the WT STAT3 protein representing the different protein domains as well as significant amino acid residues within these domains.

Figure 5. STAT3 Protein Structure



Adapted from [89]

Recently, two groups identified two non-canonical STAT pathways. In *Drosophila melanogaster*, it has been shown that the single STAT protein, STAT92E, while unphosphorylated, can mediate heterochromatin structure and stability via its association with heterochromatin protein 1 (HP-1) [61]. Subsequently, it was shown that STAT3, phosphorylated solely on the serine residue at position 727, could regulate cellular respiration in mitochondria via interactions with electron transport chain complexes I and II [62] and this function comes at the expense of its canonical transcriptional function. These discoveries are in stark contrast to the traditional view of STATs as transcription factors. While the *Drosophila* STAT protein is more closely related to STAT5, it has yet to be shown whether any of the other STATs have a similar function in *Drosophila* or in mammals.

It would seem however that the canonical view of STAT3 might not be the only function this particular protein has in the cell. In support of this idea, unphosphorylated STAT3 has a transcriptional function as well and upregulates a number of oncogenes found in various types of cancer [63]. A function for STAT4 and STAT6 was also identified in regulating chromatin activation status through regulation of epigenetic activation and repression marks [64]. STAT4 was shown to increase the histone 3 lysine 4 trimethylation (H3K4me3), known to be an activating marker; STAT6 on the other hand decreased the amount of H3K27me3, a known repression marker. Another member of the JAK/STAT pathway, namely JAK2, has also recently been identified to have a role in regulating heterochromatin structure through inhibiting the binding of heterochromatin protein 1- α (HP1- α) by phosphorylating tyrosine 41 (T41) on histone H3 (H3) leading to a more open and active chromatin conformation [65].

STAT3 and inflammation:

Due to the inability to generate genome-wide STAT3 knockout mice because of the embryonic lethality [52], it is necessary to study STAT3's function in a lineage-specific context. Hematopoietic STAT3-deficient mice have been produced [43]. These mice display mild to moderate osteoporosis [66] as well as a Crohn's disease-like phenotype characterized by increased infiltration of myeloid cells most likely responsible for the observed increase in production of inflammatory cytokines and severe deterioration of the bowel and intestinal tract [43][67].

STAT3 is important for both positively and negatively regulating inflammation. This is evidenced not only through its known activation by IL-6 [57], an inflammatory cytokine, but also through the dependence of inflammatory IL-17-producing helper T cells (TH17) on STAT3's regulation of retinoic acid receptor-related orphan receptor- γ -T (ROR γ T), a TH17-lineage specific transcription factor [68]. STAT3's anti-inflammatory role has also been well characterized. Evidence suggests this occurs primarily through IL-10, a known anti-inflammatory cytokine, whose expression is dependent on STAT3 in both mice and humans [69][70]. IL-10 also signals through STAT3 to inhibit the proliferation of macrophages [71]. STAT3 auto-regulates inflammatory cytokine signaling via induction of suppressor of cytokine signaling 3 (SOCS3), which competes with STAT3 for binding to the cytoplasmic portion of the receptor thus attenuating signaling [72]. Inflammation has not only been shown to be important in the immune system setting, but through epidemiological studies, it is evident that inflammation is a key player in oncogenesis [73][74].

STAT3 and cancer:

The link between inflammation and cancer development is an intense area of study because of the implication that targeting the immune system may lead to more effective cancer treatment and prevention [60][75]. As was noted earlier, STAT3 is an important regulator of inflammation and cellular growth control, and thus has been a focus for its role in promoting tumorigenesis. STAT3 signaling is commonly overactive in solid tumors [76][77]. The relationship between the tumor cells and tumor-associated non-transformed cells is important for cancer progression and cell survival possibly due to a STAT3 feed-forward loop [59]. STAT3 along with NF κ B are important mediators of cancer-associated inflammation [73] and persistent activation of STAT3 in immune cells leads to defective immune responses against the tumor [60].

These two molecules are important not only for the growth and survival of tumors, but also function to stimulate the epithelial-mesenchymal transition of tumors, which is the first step in their metastasis to other organs [78-80]. The effectors of this transition can be inflammatory cytokines such as IL-6, IL-1, TNF α , and transforming growth factor- β (TGF β) [78] leading to expression of NF κ B and STAT3 targets important for this transition [79][80].

STAT3 seems to have a dual role in inflammation and cancer. In non-immune cells, STAT3 functions to promote cell survival and proliferation [81]. In tumor-associated immune cells, unphosphorylated STAT3 interacts with NF κ B to produce inflammatory signals that aid the cancer cells in survival and eventual metastasis [82][83]. Moreover, in myeloid cells, STAT3 regulates cell survival, growth and function [36][42], but also is responsible for anti-inflammatory responses via inducing IL-10 expression and participating in IL-10 signaling, including suppression of TLR4-induced inflammatory gene expression [38][69][70][71].

The immunosuppressive functions of STAT3 signaling via IL-10 have been well characterized, as has its function in promoting oncogenesis through its pro-inflammatory interactions with NFκB. Recently, STAT3 has been implicated as the effector of another human syndrome whose phenotype encompasses each of the known functions for STAT3 both in inflammation and cancer.

Hyper-IgE Syndrome:

Hyper-Immunoglobulin E (IgE) syndrome (HIES), otherwise known as “Job’s Syndrome” due to the skin lesions reminiscent of the lesions of Job in the Bible’s Old Testament, is a primary immunodeficiency with both an autosomal dominant (AD) or autosomal recessive (AR) heritability pattern. The characteristic phenotype of this disease includes elevated levels of IgE in the serum, skin lesions, cold abscesses, recurrent staphylococcal infections of the skin and respiratory tract, as well as bone abnormalities affecting the spine, teeth, and long bones, specifically osteopenia (Table 1, & [84]). Several types of cancer have also been correlated with this disease [85][86][87]. Until recently, the genetic cause for this disease was unknown.

In 2007, two groups concordantly discovered the genetic basis for this disease. Multiple individual mutations in the *STAT3* gene were identified in individuals presenting with the AD form of HIES ([88][89]. The authors noted that the mutations occurred primarily in the DNA-binding domain, SH2-domain, and the TAD, and most likely affected the protein structure such that the mutant STAT3 proteins acted like dominant negatives by interfering with the wild-type STAT3 and preventing its activation or its ability to bind DNA. Since then, a fair amount of research has been focused on determining how STAT3 induces the phenotypic abnormalities associated with HIES.

Table 1. Phenotype of STAT3 deficient mice and humans with HIES

Hematopoietic <i>Stat3</i> ^{Δ/Δ} mice	Ref.	Human Hyper-IgE syndrome	Ref.
Increased inflammatory mediators in the serum	52	Elevated IgE levels in the blood	84, 90, 121
Crohn's disease-like pathology	43	Recurrent pneumonias	84, 90, 91
Increased susceptibility to endotoxin shock	52	Skin lesions/Cold Abscesses	84, 90
Osteoporosis	66	Increased inflammatory mediators in the serum	89, 84
Increased osteoclastogenesis	66	Osteopenia with pathologic fractures	90, 121
		Hyper-extensible joints	84, 90
		Scoliosis	84, 90
		Defective Th17 differentiation	92,93, 94,98
		Defective IL-10 signaling	95-96
		Increased oncogenesis	85-87

Possibly the most devastating pathology of this disease is the recurrent infections in the majority of patients. These can range from infections caused by the *Staphylococcus* and *Streptococcus* families [90] to the *Pseudomonas* and *Aspergillus* families. In most cases, these infections have been deemed the cause of death [91]. Therefore, most research to date has been focused on how the loss of STAT3 impairs the immune system in such a way as to allow these microbes to proliferate unchecked. Several groups have made key observations in this respect.

Patients with HIES have an observed lack of Th17 cells both *in vitro* and *in vivo* [92][93][94]. Given STAT3's importance for the expression of retinoid-related orphan receptor γ T (ROR γ T) [68], the loss of Th17 cells, which depends on ROR γ T for their development, makes sense. This severe lack of Th17 could play a large part in the susceptibility to fungal and bacterial pathogens found often in patients with HIES. Further evidence suggests that STAT3's function in IL-10 signaling may also be important for the imbalanced inflammatory response in patients with HIES. While lymphocyte numbers in the blood remain normal, dendritic cells (DC) were found to be unable to become tolerogenic in the presence of IL-10, as well as to induce naïve CD4⁺ T cells to becoming inducible T-regulatory cells (iTregs) [95]. DC from HIES patients were also shown to secrete more inflammatory cytokines, even in the presence of IL-10 [96].

By comparing what is known about patients with HIES and mice with hematopoietic specific deletion of *Stat3*, it is reasonable to propose that STAT3 is important for regulating bone development, immunity against bacterial and fungal pathogens, and production of NF κ B-regulated inflammatory cytokines. However, no direct evidence to date suggests how STAT3 is affecting bone development and

homeostasis, or how STAT3 is affecting NF κ B-mediated inflammatory gene expression in these two models.

Project Goal:

Traditionally, STAT3 has been considered to solely act as a transcription factor in the regulation of pathways leading to cell growth, survival, and differentiation as well as in regulation of inflammation. Although STAT3 has been shown to be important in bone development [66], little data exists elucidating the exact mechanism as to how it is involved. Data from our lab and others (H. Zhang, unpublished data)[82][97] indicates a role for STAT3 in regulating NF κ B signaling in the hematopoietic system. The goal of this project was to examine how the point mutations identified in HIES affect STAT3's function in NF κ B-mediated gene expression and by doing so, gain a more detailed understanding of the role for each domain in this regulation.

Methods

Cell Lines, Culture Conditions and Cytokine/LPS Treatments:

Primary murine macrophages were generated from total bone marrow, collected from 6-8 week old C57BL/6 mice, by culturing in DMEM containing 20% fetal calf serum (FCS) and 20% conditioned medium from L929 cell supernatants (source of M-CSF) for 3 days. Primary murine osteoclasts were then generated by addition of 50ng/mL RANKL (R&D Systems, #390-TN-010) for 4 days. RAW cells (mouse macrophage cell line) were cultured in DMEM supplemented with 10% FCS. Similarly, the STAT3-null murine embryonic fibroblast cell line (L1) was maintained in DMEM with 10% FCS. The RAW and L1 cells expressing WT STAT3 or one of the STAT3 point mutations

were generated by retroviral transduction. Briefly, 3×10^5 cells were plated in a 6-well plate and allowed to adhere for 30 minutes at 37° C. 1 mL of retrovirus was then added to 0.5 mL complete media along with 8ug/mL polybrene. Cells were spun at 2300 rpm for 1 hour, then allowed to incubate for 4 hours before media was aspirated and replaced with DMEM plus 10% FCS. Cells were subject to sorting for GFP+ cells after 48 hours. For assays involving analysis of STAT3 transcriptional activity, cells were treated with murine IL-6 (25ng/mL: R&D systems #406-ML-005) or mIL-6 plus mouse soluble IL-6 receptor alpha (sIL-6R α) (25ng/mL: R&D systems #1830-SR-025) for 30 minutes (immunoblots), 3 hours (luciferase assays), or indicated time points (quantitative real-time PCR). For primary osteoclast differentiation assay and STAT3 inhibitor quality control, cells were stimulated with 20 ng/mL recombinant human G-CSF. For inflammatory gene expression analysis, 1×10^6 RAW cells were plated in a 12 well plate in 1mL media and starved overnight in DMEM with 1% FCS. RAW cells were then stimulated with Lipopolysaccharide (LPS) (100ng/mL: Sigma #L3024) for the indicated time points. 5×10^5 L1 cells were plated in a 6 well dish and starved overnight in DMEM with 1% FCS. L1 cells were then stimulated with LPS (100 ng/mL) for indicated time points. All cells were maintained in a humidified incubator at 37° C and 5% CO₂.

STAT3 mutant generation:

STAT3 cDNAs encoding individual point mutations (R382W, V637M, and V713L) were generated by Dr. Huiyuan Zhang using the QuikChange II Site-Directed Mutagenesis kit (Stratagene, #200523) as described in the manufacturers protocol. The presence of the mutations was confirmed by DNA sequencing. The truncated STAT3 mutants were generated (TAD: X. Xie and Watowich unpublished results, Δ 133: L. Zhang [100])

using a PCR-based strategy and confirmed by gel electrophoresis and DNA sequencing.

Production of VSVg-pseudotyped MCSV-based STAT3 retroviruses:

cDNAs encoding WT STAT3 or the three HIES point mutants described previously were cloned into the pMX-IRES-GFP retroviral vectors via digestion with Sph1 and Not1 and confirmed by gel electrophoresis. Retroviruses were then generated using the 293T packaging cell line via the calcium-phosphate transfection method. Briefly, 14ug plasmid cDNA along with cDNA encoding the packaging constructs (8ug VSVg, 10ug Gag/Pol) were mixed with CaCl_2 and water. Hepes-buffered saline (HBS) was then added drop by drop to the DNA/ CaCl_2 mixture while bubbling. This mix was then allowed to sit for 5 minutes before adding drop-wise to the plate of 293T cells (60-80% confluency) in DMEM with 10% FCS and 20uM chloroquine. Cells were incubated for 8 hours and then medium was replaced with fresh DMEM plus 10% FCS. Supernatant containing viral particles was collected after 48 and 72 hours and used fresh or frozen (stored at -80°C).

STAT3 SH2 domain inhibitor:

A STAT3-specific SH2 domain inhibitor (73g) was kindly provided by Dr. John McMurray (M.D. Anderson Cancer Center). The unreconstituted inhibitor was stored at -20°C . For working concentrations, inhibitor was reconstituted in 99.9% pure DMSO at and aliquots were frozen at -80°C . For STAT3 inhibition experiments, the inhibitor was added at the indicated concentrations and replaced every 12 hours for the indicated time period.

Preparation of whole cell lysates, SDS-polyacrylamide gel electrophoresis, and immunoblot analysis:

Cells were treated as indicated (section: Cell Lines, Culture Conditions and Cytokine/LPS Treatments) and then washed with 1X PBS. Laemmli gel sample buffer (2% SDS, 80mM Tris pH 6.8, 15% Glycerol, 0.01% Bromophenol Blue, 1% Betamercaptoethanol) was added and the cell pellet was sonicated and boiled (10 minutes, 100°C) for whole cell lysates. 5×10^5 (Raw)/ 2.5×10^5 (L1) cell equivalents were separated on 10-15% SDS-polyacrylamide gels by electrophoresis. Protein was then electrophoretically transferred to a nitrocellulose membrane for antibody staining. Membranes were briefly washed in ddH₂O and then blocked for 1 hour at room temperature. For phosphorylated STAT3, 5% BSA in TBST (1X TBS, 0.05% Tween-20) was used for blocking. For total STAT3 and RAN, 5% milk in PBST (1X PBS, 0.05% Tween-20) was used. For total and phosphorylated JNK, 5% milk in TBST was used for blocking. For Tubulin, 1% BSA in TBST was used for blocking. Membranes were then incubated overnight at 4° C with primary antibodies in their respective diluents: Phosphorylated STAT3 (1:1000 in 5% BSA-TBST, Cell Signaling #9131S), STAT3 (C-20/H-190, 1:1000 in 5% milk-PBST, Santa Cruz Biotechnologies, #SC-482 & SC-7179), Phosphorylated JNK (1:500 in 5% BSA-TBST), total JNK1 (1:500 in 5% milk in PBST), Tubulin (1:1000 in 1% BSA-TBST, Sigma #T9026), Ran (1:1000 in 5% milk-PBST, Santa Cruz Biotechnology, #SC-1156). After overnight incubation, membranes were washed with PBST three times followed by addition of secondary antibody for incubation at room temperature for 2 hours (pSTAT3/STAT3/pJNK, anti-rabbit IgG-HRP, GE-life sciences #NA934; Tubulin/JNK1, anti-mouse IgG-HRP, GE-life sciences #NA9310; and for Ran, anti-goat IgG-HRP, Santa Cruz #SC-2020, were

used). Membranes were washed 3 more times in PBST followed by development using West Pico Substrate (Thermo Scientific, #34087).

Quantitative Real-time polymerase chain reaction (qPCR):

Cells were treated as indicated and then lysed in Trizol Reagent (Molecular Research Center, #TR118). Total RNA was extracted per the manufacturer's protocol and RNA concentration was analyzed on a Nanodrop-1000. 1ug of total RNA was subjected to reverse transcriptase PCR (RT-PCR) using the IScript system (Biorad, #1708891). cDNA was diluted 1:5 and 5uL was used for each sample in qPCR. Samples were combined in a 20uL mixture containing nuclease-free water, specific oligonucleotides, and iQ SYBR Green mastermix (Biorad, #1708882). Each sample was run in duplicate on a Biorad C1000 Thermal Cycler CFX96 Real-time system. PCR conditions were: 95°C 3 min, (95°C 10 seconds, 59°C 20 seconds, 72°C 30 seconds) X 39 cycles. Samples calculations were relative to an internal control, 18s rRNA. Data were analyzed using the $\Delta\Delta C_t$ method in Microsoft Excel using the formula [Relative expression level= $\text{power}(1.8, (\text{Control } C_t \text{ value} - \text{Target } C_t \text{ value})) \times 10^7$]. P values were calculated using either Student's *t*-test or 2-way ANOVA with a Bonferroni post-test.

Oligonucleotide sequences for qPCR:

Please see Table 2

Transient Transfection for STAT3 overexpression:

293T cells were grown to 60-80% confluency prior to transfection. 10ug of DNA was transiently transfected using the calcium phosphate method described in section: Production of VSVg-pseudotyped MCSV-based STAT3 retroviruses. Cells were incubated with DNA precipitate and 20uM chloroquine in DMEM plus 10% FCS for 6 hours and then the media was replaced. Cells were then incubated for 48 hours before analysis by immunoprecipitation and immunoblotting.

Table 2. Sequences of qPCR oligonucleotides

	Forward (5'→3')	Reverse (5'→3')
IL-6	CTGATGCTGGTGACAACCAC	CAGAATTGCCATTGCACAAC
IP-10	CCCACGTGTTGAGATCATTG	GAGGCTCTCTGCTGTCCATC
IL-1b	AAGCCTCGTGCTGTCGGACC	TGAGGCCCAAGGCCACAGGT
TRAP	CGTCTCTGCACAGATTGCAT	GTAGTCCTCCTTGGCTGCTG
CSK	CCAGTGGGAGCTATGGAAGA	AAGTGGTTCATGGCCAGTTC
CALC	CGGACTTTGACACAGCAGAA	GTCACCCCTCTGGCAGCTAAG
SOCS3	GAGATTTGCTTCGGGACTA	GCTGGTACTCGCTTTTGGAG
Myc	ACAATCTGCGAGCCAGGACA	CCAACGCCCAAAGGAAATCCA
MIP-2	AAGTTTGCCTTGACCCTGAA	AGGCACATCAGGTACGATCC
TNFa	GAACTGGCAGAAGAGGCACT	AGGGTCTGGGCCATAGAACT
GAPDH	CTCATGACCACAGTCCATGCCATC	CTGCTTCACCACCTTCTTGATGTC
B-actin	AGCCATGTACGTAGCCATCC	TTTGATGTCACGCACGATTT
18s rRNA	CGCGGTTCTATTTTGTGGT	AGTCGGCATCGTTTATGGTC

Flag-immunoprecipitation and immunoblotting:

10-20x10⁶ cells were pelleted and washed with 1X PBS containing a protease inhibitor cocktail (Roche, #11873580001) and placed on ice. Pellets were lysed in 0.5mL non-denaturing isotonic triton lysis buffer (1% Triton X-100, 50mM Tris-Cl pH 7.4, 300mM NaCl, 5mM EDTA, 0.02% Sodium Azide) containing the protease inhibitor cocktail (Roche) on ice for 5 minutes. Lysates were spun at 14,000 RPM at 4° C for 15 minutes. Supernatants were collected and 20uL Protein-G agarose beads (Santa Cruz Biotechnology, #SC-2002) was added to pre-clear lysate of non-specifically bound proteins. Samples were rotated at 4° C for 1 hour. Samples were then spin to remove cell debris and supernatants were collected. Protein concentration was detected and normalized between samples. One-tenth of the total volume was removed to use for the input controls. 2uL of anti-Flag M2 antibody (Sigma, #F3165) were then added and samples were rotated overnight at 4° C. Then Protein-G agarose beads (40uL) were added and samples continued to rotate at 4° C for 1 hour. Samples were spun and supernatants were discarded. Beads were washed 3X with isotonic Triton lysis buffer containing protease inhibitor and 1X with PBS containing protease inhibitor and then resuspended in 40uL Lammeli sample buffer and boiled for 10 minutes. 40uL immunoprecipitated and input samples were run on a 15% polyacrylamide gel and electrophoretically separated and STAT3 expression was analyzed by immunoblot.

Transfection of STAT3-deficient mouse embryonic fibroblasts for Luciferase assay

1x10⁴ STAT3^{-/-} MEFs were plated in duplicate per well of a 48 well plate in 0.2 mL complete DMEM the night before transfection. On the following day, cells were transfected using Lipofectamine LTX and PLUS reagent (Invitrogen #15338030) according to the manufacturers protocol. Briefly, 0.4ug of total DNA was diluted in 40 uL serum free media per well. PLUS reagent (0.4uL) was added to the diluted DNA

and incubated at room temperature for 15 minutes. Lipofectamine LTX was added (0.2uL) to DNA:PLUS mixture, and incubated for 30 minutes at room temperature. Finally, 40 uL/sample was added to each well of the 48-well plate and incubated for 40-48 hours. The ratio of DNA to lipid was optimized according to the manufacturers optimization protocol.

Luciferase assays

Transfected STAT3-deficient mouse embryonic fibroblasts were assayed for luciferase activity using the Promega Dual-luciferase reporter kit following an amended manufacturers protocol. After a 3 hour stimulation with 25ng/mL IL-6 and 25ng/mL sIL-6R α , cells in a 48-well plate were lysed with passive lysis buffer for 15 minutes at room temperature. 5 uL lysate per sample was mixed with 5uL luciferase assay reagent II and then the firefly luciferase was read using a Sirius Luminometer from Burthold Detection systems. Stop and Glo reagent was added (5uL) and the background renilla luciferase activity was detected. Each sample was transfected in duplicate, and then averaged before being normalized to the average renilla luciferase reading.

Results:

Generation of the STAT3 mutant constructs

STAT3 contains 5 distinct protein domains: N-terminal region, coiled-coiled domain, DNA-binding domain, SH2-domain and C-terminal transactivation domain (TAD). Traditionally the DNA-binding region, SH2 domain, and TAD are considered to be important for STAT3's function as a transcription factor, whereas the others may be involved in protein-protein interactions [53].

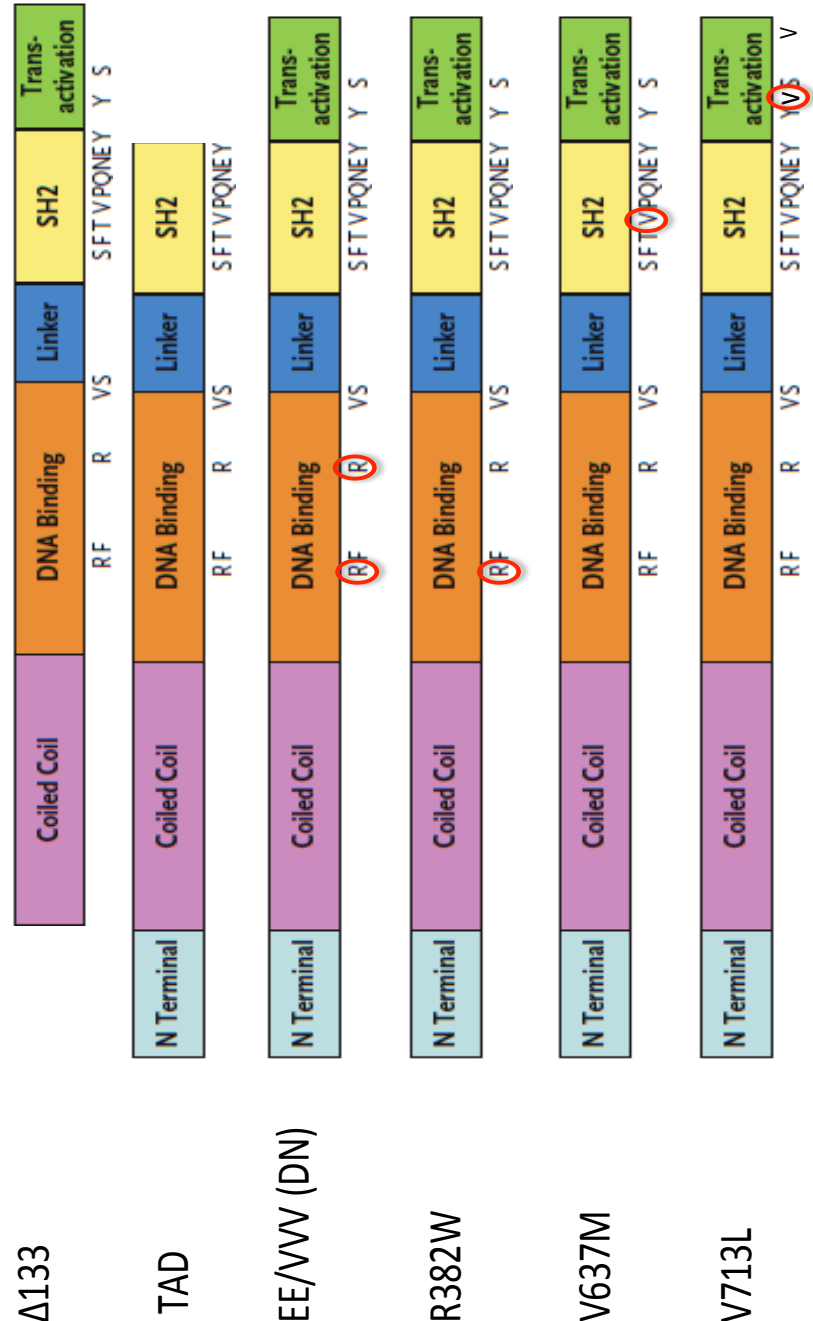
To evaluate how STAT3 functions in osteoclastogenesis and inflammatory gene expression, we first generated STAT3 constructs containing mutations in each of these

domains (Fig. 6). Previous members of our lab generated an N-terminal truncated form of STAT3, termed $\Delta 133$ for the loss of the first 133 amino acid residues [100], as well as a construct that lacks the entire transactivation domain at the C-terminus [X. Xie and S. Watowich, unpublished results]. These were generated via a polymerase chain reaction (PCR)-based strategy. A published construct, EE/VVV, was provided by Drs. Curt Horvath and Jim Darnell, and has been shown to elicit dominant negative activity [54]. Finally, we chose three of the published point mutations identified in patients with HIES (R382W, V637M, and V713L) and generated them via site-directed mutagenesis [H. Zhang and S. Watowich, unpublished results]. R382W is located within the DNA-binding domain and is predicted to function similarly to the EE/VVV mutant by allowing STAT3 phosphorylation and dimerization but preventing its binding to promoter elements on the DNA. V637M is located within the SH2-domain, and published reports show that it lacks the ability to become tyrosine phosphorylated after EGF stimulation of transiently transfected COS-7 cells [98]. V713L is found in the transactivation domain but adjacent to the SH2 domain in tertiary protein structures as seen through virtual protein modeling [E. Ohashi and S. Watowich, unpublished results]. While there are no reports on how this mutation affects STAT3 signaling, we hypothesize that it will act similarly to the V637M mutation due to its proximity to the SH2 domain and the important tyrosine residue at position 705.

To confirm that these constructs were expressed *in vitro*, we transiently transfected 293T cells with plasmids encoding each mutant, all containing in-frame C-terminal FLAG epitope tags, and evaluated their expression by immunoprecipitation with anti-FLAG antibodies and immunoblotting for total STAT3. We found that each construct was expressed at relatively similar levels, excluding the EE/VVV and TAD mutants (Fig. 7). Each mutant construct was expressed from a green fluorescent

Figure 6. Schematic representation of the various STAT3 mutants we and others generated to analyze the function of the different domains and point mutants in HIES. Red circles denote the specific amino acids mutated in each construct.

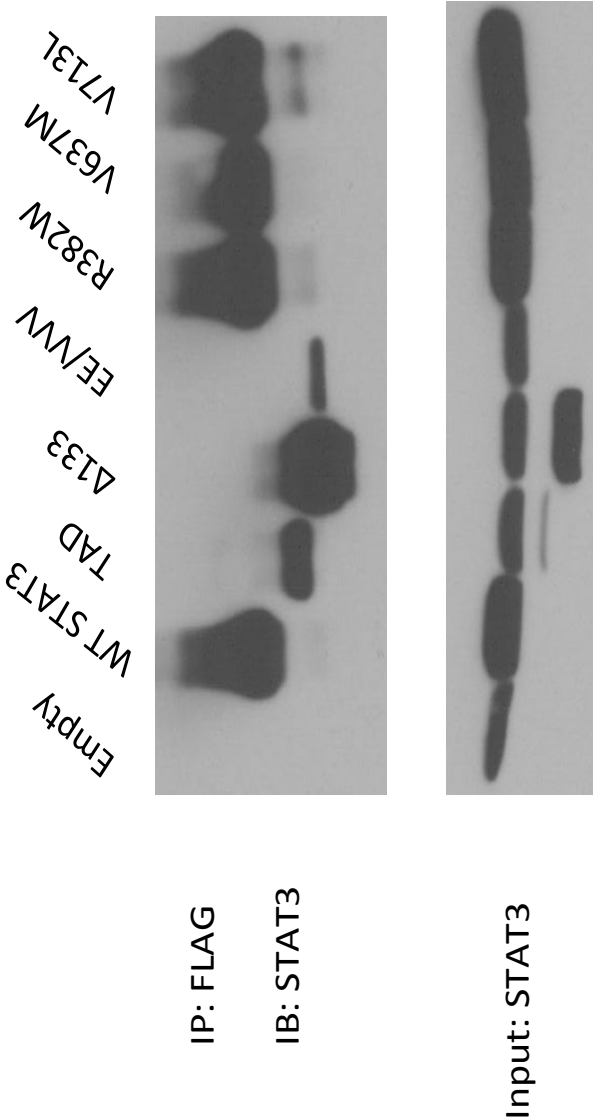
Figure 6. STAT3 Truncation and HIES mutants



○ Mutated amino acid

Figure 7. Transient overexpression of the STAT3 mutants in 293T cells. Total cell lysates were immunoprecipitated with anti-FLAG antibodies and then immunoblotted for total STAT3. A portion of lysate before immunoprecipitation (Input) was examined for total STAT3 expression and RAN as a loading control.

Figure 7. Transient expression of STAT3 mutants in 293T cells



protein (GFP)-containing vector to assist us in tracking the expression of mutant proteins throughout our experiments. Prior to each experiment, the GFP expression was checked via fluorescent microscopy and multiple times throughout the project a confirmatory immunoblot was run to verify continued expression of the mutants. Based on this result, we chose to focus on comparing wild-type (WT) STAT3 with the three HIES point mutations in our studies.

Effects of HIES mutants upon phosphorylation of endogenous STAT3

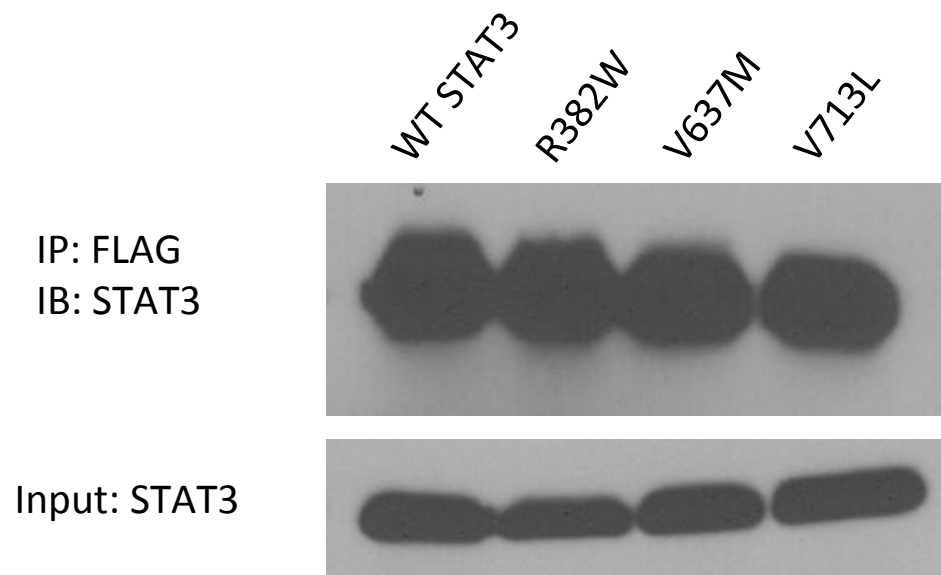
The STAT3 mutations identified in patients with HIES have been assumed to be dominant negative due in part to the heterozygosity of HIES patients as well as *in vitro* assays performed with mutated STAT3 isoforms in cell culture systems [88]. The dominant negative action of mutated STAT3 in HIES is proposed to lead to the severe clinical defects with this syndrome including osteopenia, increased incidence of infection, and high IgE serum levels. However, of the three mutations we were interested in, only the mutation located in the DNA-binding domain (R382W) has been assayed for dominant negative activity via luciferase assays [88][89]. We wanted to determine whether the other mutations, V637M and V713L, also elicited dominant negative inhibition of STAT3 function.

We initially utilized retroviral transduction to express each mutant in a murine macrophage cell line (RAW cells). To confirm the expression of the mutants in our system, we performed immunoprecipitation and immunoblotting assays with FLAG and STAT3 antibodies, respectively. We found that each mutant was expressed at equal amounts (Fig. 8).

To determine if the mutants affect activation of endogenous STAT3, we stimulated RAW cells expressing each mutant with soluble IL-6 (sIL-6) for 30 minutes

Figure 8. Stable overexpression of WT STAT3 and STAT3 HIES mutants in murine macrophage cell line, RAW. Total cell lysates were immunoprecipitated with anti-FLAG antibodies then immunoblotted for total STAT3. A portion of lysate before immunoprecipitation (Input) was examined for total STAT3 expression and RAN as a loading control.

Figure 8. Stable overexpression of STAT3 HIES mutants in murine macrophage cell line, RAW



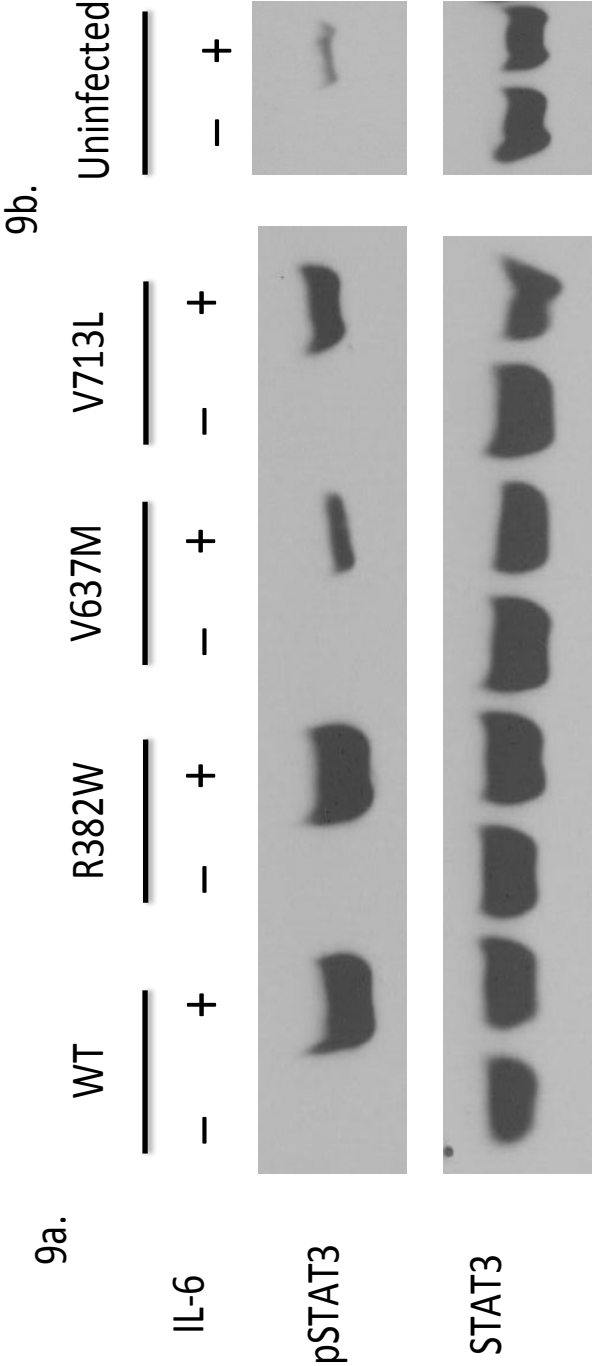
and then examined STAT3 tyrosine phosphorylation by immunoblotting. We found total STAT3 tyrosine phosphorylation amounts were similar or slightly higher in cells expressing the R382W mutant (mutated in the DNA-binding domain), compared to cells with WT STAT3 overexpression (Fig. 9a). By contrast, overexpression of the V637M mutation significantly diminished the level of STAT3 tyrosine phosphorylation compared to WT STAT3. The level of this tyrosine phosphorylation was similar to the level of tyrosine phosphorylation observed in uninfected RAW cells stimulated with sIL-6 (Fig. 9b). Importantly, cells expressing the V713L mutation, which is located in the TAD but adjacent to the SH2 domain, showed a slightly increased amount of total STAT3 tyrosine phosphorylation compared to uninfected macrophages, while exhibiting significantly less compared to cells overexpressing WT STAT3 (Fig. 9a). Together these data suggest that the mutations in the SH2 domain and TAD affect STAT3 tyrosine phosphorylation, whereas mutations in the DNA-binding domain do not.

Activation of STAT3 HIES mutants

Due to our data examining total STAT3 tyrosine phosphorylation when overexpressing the HIES mutants, we intended to identify whether the mutants alone could become activated via IL-6 stimulation. Previous studies have shown that in transiently transfected COS-7 cells, epidermal growth factor (EGF) stimulation induced STAT3 tyrosine phosphorylation in cells transiently transfected with both WT STAT3 and the R382W mutant STAT3, but not in cells expressing the V637M mutant [98]. We sought to confirm this observation within cells stably expressing the STAT3 HIES mutants in the absence of endogenous or overexpressed WT STAT3, under IL-6

Figure 9. IL-6 induced STAT3 tyrosine phosphorylation in RAW cells expressing the STAT3 HIES mutants. (a) Western blot of total cell lysates of RAW cells overexpressing the different STAT3 HIES mutants stimulated with or without 25 ng/mL sIL-6 for 30 minutes. Total STAT3 and RAN immunoblots are included as loading controls. (b) Western blot of uninfected RAW cells unstimulated or stimulated with 25 ng/mL sIL-6 for 30 minutes to examine the level of endogenous STAT3 phosphorylation.

Figure 9. IL-6 induced STAT3 tyrosine phosphorylation in RAW cells overexpressing the STAT3 HIES mutants



stimulation conditions, as well as shedding light on the activation ability of the V713L mutant, which has not been tested to date.

Using STAT3-deficient MEFs, we stably reconstituted each STAT3 HIES mutant. To confirm that the mutants were expressed, and that the parental cells were truly STAT3-deficient, we examined total STAT3 protein expression by immunoblotting. Uninfected cells and cells infected with a GFP-containing empty vector (referred to as GFP-empty vector henceforth) were used as negative controls, while 293T cells were used as a positive control (Fig. 10). We found that the HIES mutants showed similar expression levels. The uninfected and GFP-empty infected cells confirmed a lack of STAT3 expression in STAT3-deficient MEFs. By contrast, the TAD, Δ 133, and EE/VVV mutants were expressed at significantly lower amounts versus the HIES point mutants.

To examine directly the phosphorylation potential of the STAT3 HIES mutants, we used a combination of sIL-6 and soluble IL-6 receptor- α (sIL-6R α ; STAT3-deficient MEFs do not express IL-6R α) to stimulate reconstituted STAT3-deficient MEFs for 30 minutes and then assayed for STAT3 tyrosine phosphorylation by immunoblotting (Fig. 11). Consistent with our data from the RAW cells, we found increased tyrosine phosphorylation in cells expressing the R382W mutant compared to cells expressing WT STAT3. We also confirmed previous reports showing the complete lack of tyrosine phosphorylation of the V637M mutant [98]. Interestingly, we found that the V713L mutant was phosphorylated following IL-6 stimulation; however, this appeared to occur less efficiently than the WT and R382W mutants when total STAT3 level was taken into account. Together these data indicate that the mutation in the DNA-binding domain does not inhibit tyrosine phosphorylation of STAT3 but rather enhances it (Fig. 9 & 11). The SH2-domain mutation completely abrogates phosphorylation of this

Figure 10. Stable overexpression of WT STAT3 and STAT3 mutants in a STAT3-deficient MEF cell line. Whole cell lysates were immunoblotted for total STAT3 and RAN as a loading control. 293T cell whole cell lysate was used as a positive control. Non-infected and GFP-empty vector infected cells were used as negative controls.

Figure 10. STAT3 HIES mutant overexpression in STAT3-deficient MEFs

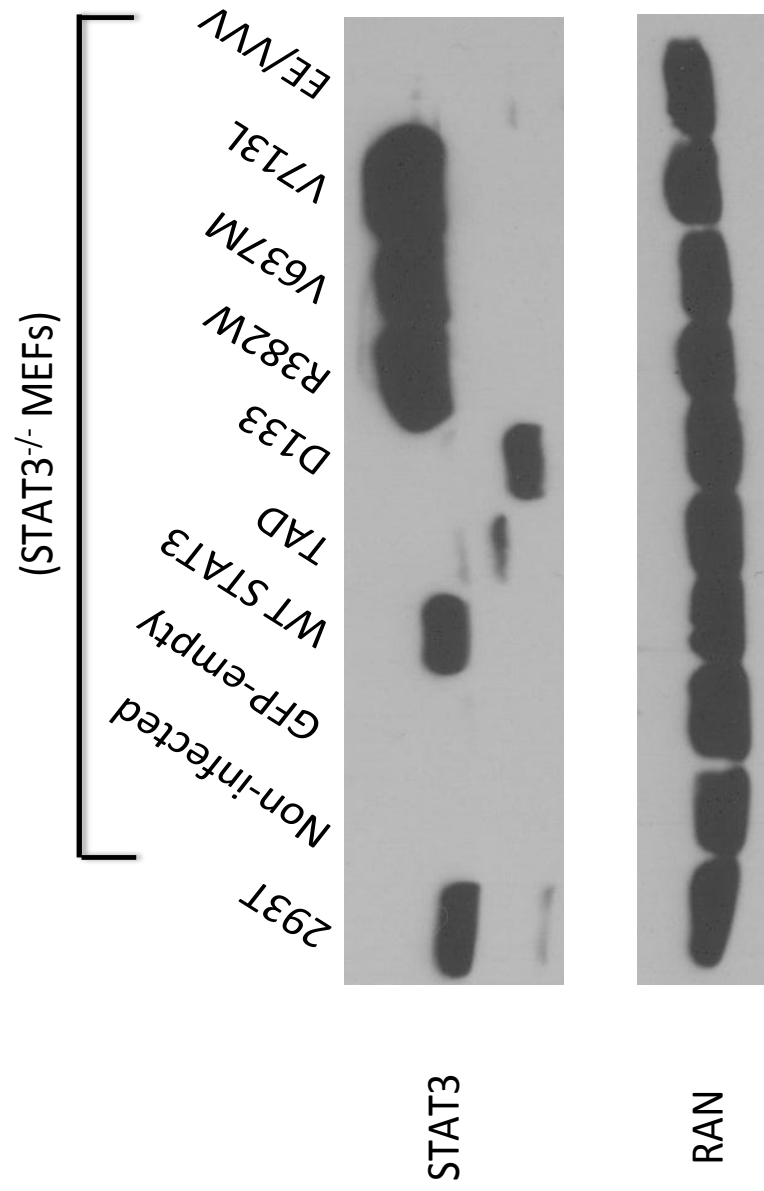
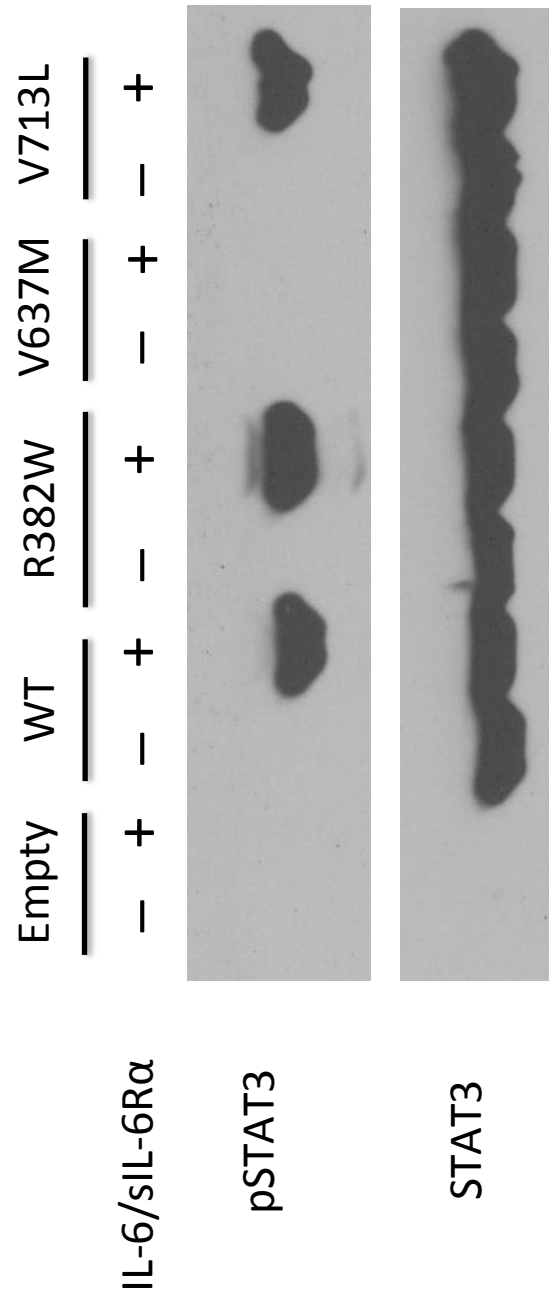


Figure 11. IL-6 induced STAT3 tyrosine phosphorylation in STAT3-deficient MEFs expressing the STAT3 HIES mutants. The STAT3-deficient MEF cell line stably expressing the STAT3 HIES mutations were unstimulated or stimulated with 25 ng/mL sIL-6 and 25 ng/mL sIL-6R α for 30 minutes and then whole cell lysates were examined by western blot of tyrosine phosphorylated STAT3 and total STAT3 expression. Ran was used as a loading control.

Figure 11. IL-6/sIL-6R α induced STAT3 tyrosine phosphorylation in STAT3-deficient MEFs stably expressing the STAT3 HIES mutants



mutant, and the TAD mutation allows STAT3 to be phosphorylated albeit at a much lower level compared to WT.

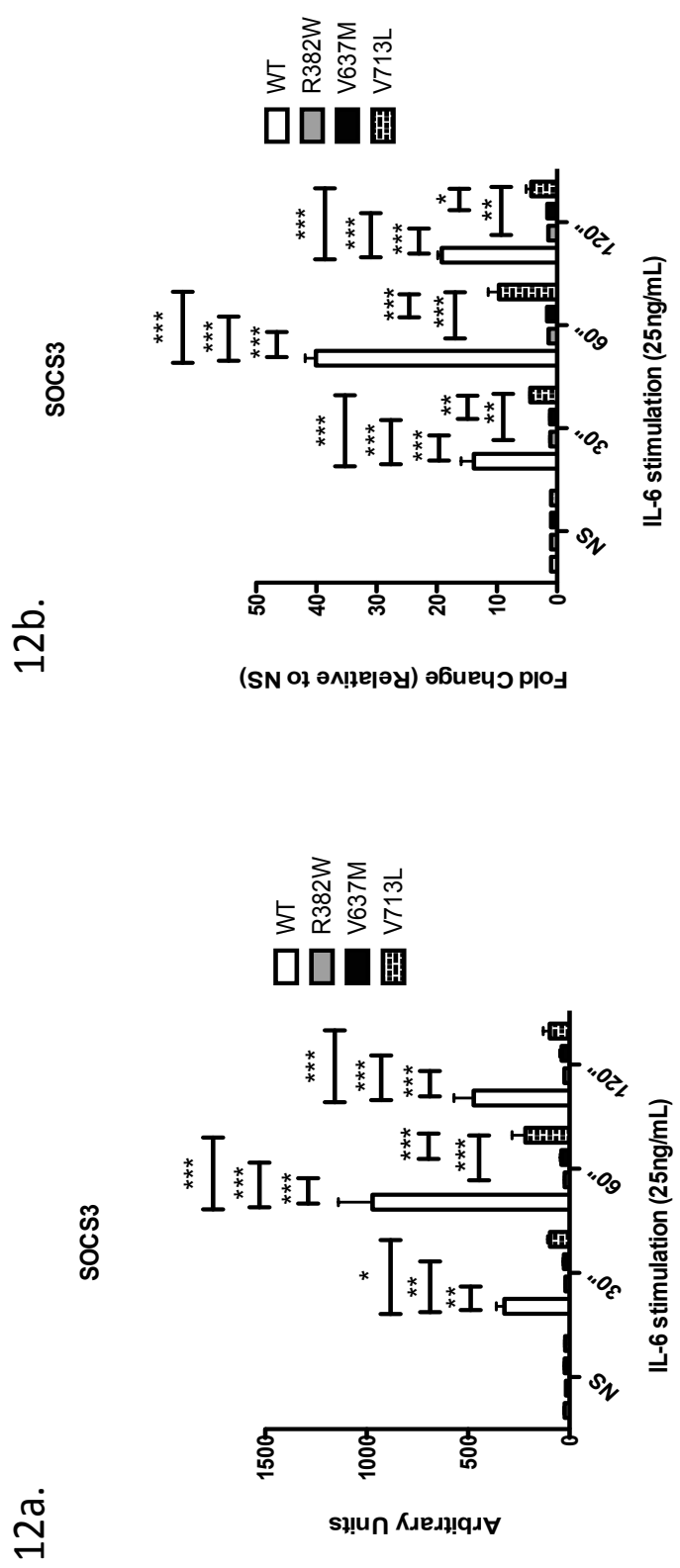
Transcriptional activity of STAT3 HIES mutants

Next, we sought to identify whether the STAT3 HIES mutants were able to exhibit transcriptional activity. The suppressors of cytokine signaling (SOCS) proteins are competitive inhibitors of JAK/STAT signaling, which act via competition for binding to the tyrosine residues of gp130 [99]. The *Socs3* promoter has been shown to contain a STAT3 binding site [100][101] and it is induced by STAT3 activation whereby SOCS3 potentially inhibits further STAT3 activation after cytokine stimulation [101][102].

To analyze the transcriptional activity of the HIES mutants after IL-6 stimulation, we treated STAT3-deficient MEFs, reconstituted with the mutants, with sIL-6 and sIL-6R α . We then analyzed *Socs3* mRNA expression at different time points by qPCR. *Socs3* mRNA expression peaked at 30 minutes of IL-6/sIL-6R α treatment (Fig. 12a) and was induced up to 40 fold (Fig. 12b) in WT cells. Figure 12a depicts the expression level of *Socs3* RNA relative to an internal control gene. Figure 12b depicts the fold change of *Socs3* RNA relative to the unstimulated control. In contrast, IL-6-responsive *Socs3* expression was significantly reduced in cells expressing the HIES mutants ($p < 0.001$) compared to WT STAT3, with cells expressing the R382W and V637M mutants displaying no *Socs3* induction compared to unstimulated samples ($p < 0.001$). The V713L mutant elicited expression of *Socs3*, which was increased by 10 fold in comparison to the R382W and V637M mutants ($p < .001$). However, this induction was still much diminished in comparison to *Socs3* expression in WT STAT3 cells. The *Socs3* expression kinetics with the V713L mutant mirrored the expression pattern of *Socs3* in WT STAT3 cells, with peak expression at 60 minutes post-

Figure 12. IL-6 induced Socs3 expression in STAT3-deficient MEFs expressing the STAT3 HIES mutants. The MEFs were unstimulated or stimulated with 25 ng/mL sIL-6 and 25 ng/mL sIL-6R α for 30, 60, or 120 minutes and then total RNA was extracted, converted to cDNA, and Socs3 mRNA expression was analyzed by qPCR. (a) Relative expression shown as arbitrary units normalized to the relative expression of 18s rRNA. (b) Fold change relative to the non-stimulated (NS) sample for each mutant. Data are mean \pm s.e.m, * p <0.05, ** p <0.01, *** p <0.001. Analyzed using a 2-way ANOVA followed by a Bonferroni post-test.

Figure 12. IL-6 induced Soccs3 expression in STAT3-deficient MEFs expressing the STAT3 HIES mutants



stimulation. These data indicate that the DNA-binding and SH2-domain mutations completely abolished STAT3's transcriptional ability, whereas the V713L mutation did not. However, the level of transcriptional activity of the V713L mutant was significantly lower level than the WT cells. This correlates well with the partially decreased phosphorylation of the V713L mutant seen in both RAW and STAT3-deficient MEFs (Figs. 9 and 11).

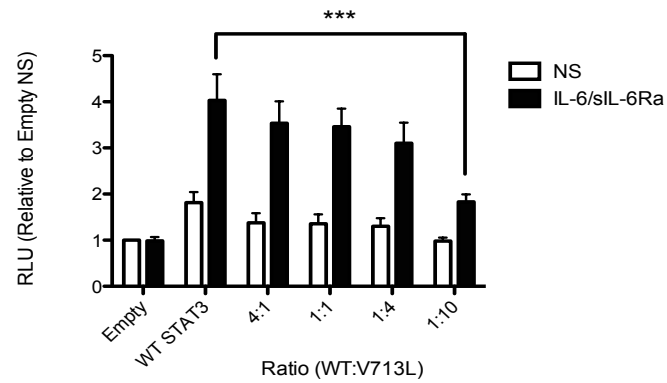
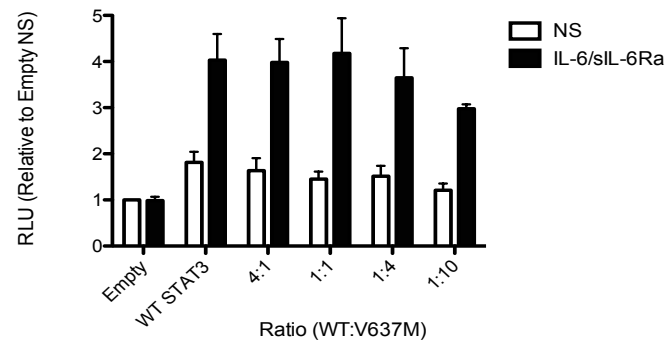
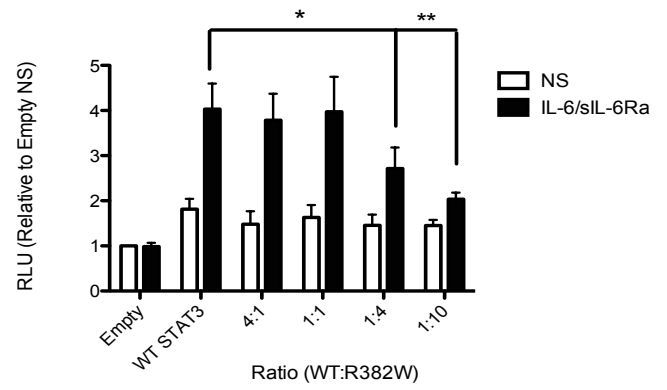
Dominant negative effects of STAT3 HIES mutants

While it is clear that each HIES mutation we tested severely diminishes the intrinsic transcriptional ability of the mutants of STAT3 (Fig. 12), it remained to be determined whether these mutations interfere with the transcriptional function of WT STAT3 thereby exhibiting proposed dominant negative activity. It has been shown that the R382W mutant does decrease STAT3 gene reporter activity in transiently transfected HepG2 cells after IL-6 stimulation [88]. Therefore we intended to confirm the dominant negative activity of this mutation and examine the activity of the V637M and V713L mutations as well.

Using STAT3-deficient MEFs, we transiently expressed WT STAT3 with a GFP-empty vector or vectors encoding the HIES mutants, in different WT:mutant ratios, along with a STAT3 reporter plasmid containing 3 consecutive STAT3 consensus binding sites upstream of the firefly luciferase gene. After 48 hours, we stimulated the cells with IL-6 and sIL-6R α and then assayed 3 hours later for luciferase activity using the Dual-luciferase reporter assay system, to measure STAT3 transcriptional activity (Fig. 13). WT STAT3 alone stimulated a 2-3 fold increase in STAT3 reporter activity in response to IL-6/sIL-6R α , relative to the empty vector non-stimulated samples. The R382W mutant significantly reduced STAT3 reporter activity by 2-fold at a 4:1 ratio to

Figure 13. The dominant negative activity of STAT3 containing the HIES mutations. The STAT3-deficient MEF cell line was transiently transfected with a STAT3 consensus reporter, an GFP-empty vector or WT STAT3 and each HIES mutant in varying ratios to WT. Cells were stimulated with 25 ng/mL sIL-6 and 25 ng/mL sIL-6R α for 3 hours and firefly luciferase activity was quantified. Data represent mean \pm s.e.m., * $p < 0.05$, ** $p < 0.01$, *** $p < 0.001$ using a 2-way ANOVA and Bonferroni post-test. Firefly values were normalized to a renilla luciferase control, values displayed are normalized to the non-stimulated empty vector sample.

Figure 13. Luciferase assay examining dominant negative activity of STAT3 HIES mutants in STAT3-deficient MEFs

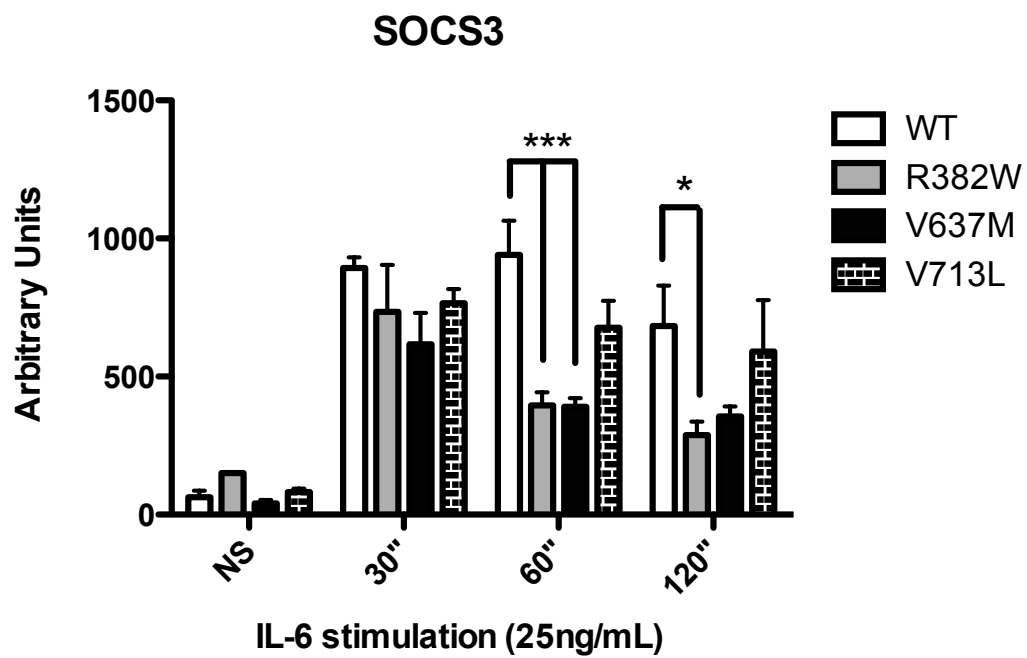


WT ($p < .05$), and approximately 3 fold at a 10:1 ratio ($p < 0.01$). The V713L mutation, also showed a trend toward dominant negative activity at a 4:1 ratio to WT, and significantly reduced STAT3 reporter activity at a 10:1 ratio with WT ($p < 0.001$). Surprisingly, the mutation located in the SH2 domain, which led to a complete lack of phosphorylation and lack of transcriptional activity, failed to significantly diminish STAT3 reporter activity, although there was a decrease of reporter activity at a 10:1 ratio with WT (Fig. 13).

To further examine the dominant negative activity of these mutants in a less artificial setting, we examined the relative level of *Socs3* mRNA after IL-6 stimulation in RAW cells stably expressing each of the HIES mutants. We stimulated these cells for 30, 60, or 120 minutes and then assayed *Socs3* mRNA expression by qPCR (Fig. 14). *Socs3* expression peaked at 30 minutes in cells overexpressing WT STAT3, and stayed elevated even at 2 hours post-stimulation. When each HIES mutant was stably overexpressed, the *Socs3* mRNA expression had similar expression kinetics, peaking at 30 minutes post-stimulation. However, *Socs3* expression was significantly decreased in comparison to WT STAT3 ($p < .001$) at 60 minutes for the R382W and V637M mutants. The V713L mutant, on the other hand, never resulted in significantly lower *Socs3* expression compared to WT STAT3. Additionally at 2 hours, the R382W mutant maintained significantly decreased *Socs3* mRNA expression ($p < .05$) whereas the V637M mutant did not, although *Socs3* expression was still low compared to WT. Together, these data suggest that the DNA-binding domain, SH2 domain, and TAD mutations impart a dominant negative ability upon STAT3, although differences appear to exist in their effects depending on the assay system used.

Figure 14. SocS3 expression after sIL-6 stimulation in macrophages expressing the STAT3 HIES mutants. The RAW cells stably expressing the STAT3 HIES mutations were unstimulated or stimulated with 25 ng/mL sIL-6 for 30, 60, or 120 minutes and total RNA was extracted and converted to cDNA. cDNA was then analyzed for SOCS3 expression by qPCR. Data are mean \pm s.e.m, * $p < 0.5$, ** $p < 0.001$ using a 2-way ANOVA and Bonferroni post-test. Values are represented as arbitrary units relative to 18s rRNA.

Figure 14. IL-6 induced *Socs3* expression in RAW cells overexpressing the STAT3 HIES mutants



Effect of STAT3 function on osteoclast-specific gene expression

In addition to determining whether specific HIES mutations were inhibiting STAT3's function via interfering with its phosphorylation or transcriptional ability, we sought to further examine how these mutations affected the function of STAT3 in phenotypes observed in both hematopoietic STAT3-deficient mice and patients with HIES.

Upon exposure to RANKL, cells of the monocyte/macrophage lineage begin to differentiate into osteoclasts [103]. RANKL stimulation results in the activation of NFκB [104], and osteoclast differentiation is NFκB dependent [17]. As these cells further differentiate from the precursors to mature activated osteoclasts, they up-regulate expression of genes specific for their function, which include, but are not limited to *Acp5/ACP5* (TRAP), *Ctsk/CTSK* (CSK), and *Calcr/CALCR* (CALC) (Fig 1b)[15][16].

We originally sought to investigate whether and how STAT3 regulates osteoclast differentiation using RAW cells, which have been shown to undergo RANKL-responsive osteoclast differentiation [105-108], however we had difficulties inducing sufficient differentiation of these cells. Therefore, we obtained a small molecule STAT3 inhibitor from Dr. John McMurray at M. D. Anderson Cancer Center. This inhibitor functions as an antagonist for the SH2-domain of STAT3. By physically interacting with this domain, the inhibitor should not only prevent STAT3's interaction with the phospho-tyrosine on the cytoplasmic domain of the STAT3-activating receptor thereby inhibiting its tyrosine phosphorylation, but also prevent dimerization and subsequent activation, very much similar to how we hypothesize the V637M mutation affects STAT3. To verify the effect of the inhibitor on STAT3 tyrosine phosphorylation, we isolated total bone marrow from C57BL/6J mice and stimulated cells with granulocyte-colony stimulating factor (G-CSF), a STAT3-activating cytokine, in the

presence of increasing concentrations of the STAT3 inhibitor. Since the inhibitor was dissolved in dimethylsulfoxide (DMSO), we used DMSO treatment for 30 minutes as a control. We examined cell lysates by immunoblotting for tyrosine phosphorylated STAT3, total STAT3, and α -tubulin, with that latter serving as a loading control (Fig. 15a). These assays showed that as the concentration of the inhibitor increased, the amount of STAT3 tyrosine phosphorylation substantially decreased and eventually was undetectable. As expected, the inhibitor had no effect on the relative abundance of STAT3 protein, as the amount of total STAT3 remained the same.

Next, we cultured total murine bone marrow from C57BL/6J mice in the presence of conditioned medium containing macrophage-colony stimulating factor (M-CSF) for 3 days to generate bone marrow-derived macrophages. The macrophages were subsequently cultured for 4 days in the presence of RANKL with varying concentrations of the STAT3 inhibitor. The gene expression of the three osteoclast-specific genes was analyzed by quantitative real-time PCR (qPCR)(Fig. 16). We found that with increasing concentrations of inhibitor, and thus less activated STAT3, the expression of *Acp5* (TRAP), *Ctsk* (CSK), *Calcr* (CALC) were all significantly up-regulated. This indicates a role for the STAT3 SH2-domain, as well as activated STAT3, in the negative regulation of osteoclast differentiation and expression of genes important for osteoclast function.

Analysis of the effect of the HIES mutations on inflammatory gene expression in mouse macrophages stimulated with LPS

NF κ B activity is not only important for osteoclastogenesis, but is also highly involved in the inflammatory response [19][20][21]. To determine whether STAT3 is involved in another NF κ B-mediated pathway, and whether the HIES point mutations

Figure 15. STAT3 and STAT5 G-CSF induced phosphorylation in the presence of a STAT3 inhibitor. Total murine bone marrow were isolated from C57BL/6J mice and stimulated with 20 ng/mL granulocyte colony stimulating factor (G-CSF) +/- an antagonistic inhibitor for the STAT3 SH2 domain at 50, 500, or 5000 ng/mL. Whole cell lysates were analyzed by western blot examining (a) p-STAT3, total STAT3, (b) p-STAT5 and total STAT5 expression. α -tubulin was used as a loading control.

Figure 15. G-CSF induced STAT3 and STAT5 phosphorylation of murine bone marrow in the presence of a STAT3 inhibitor

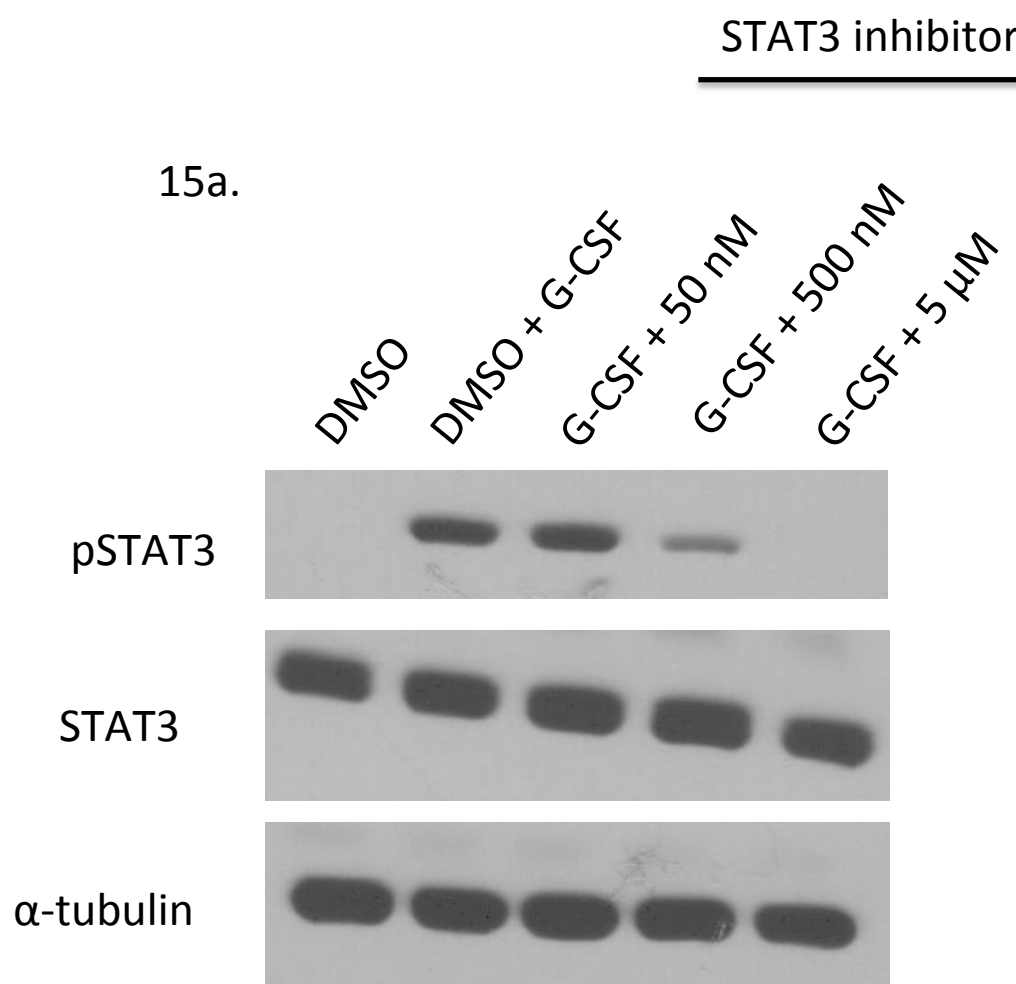
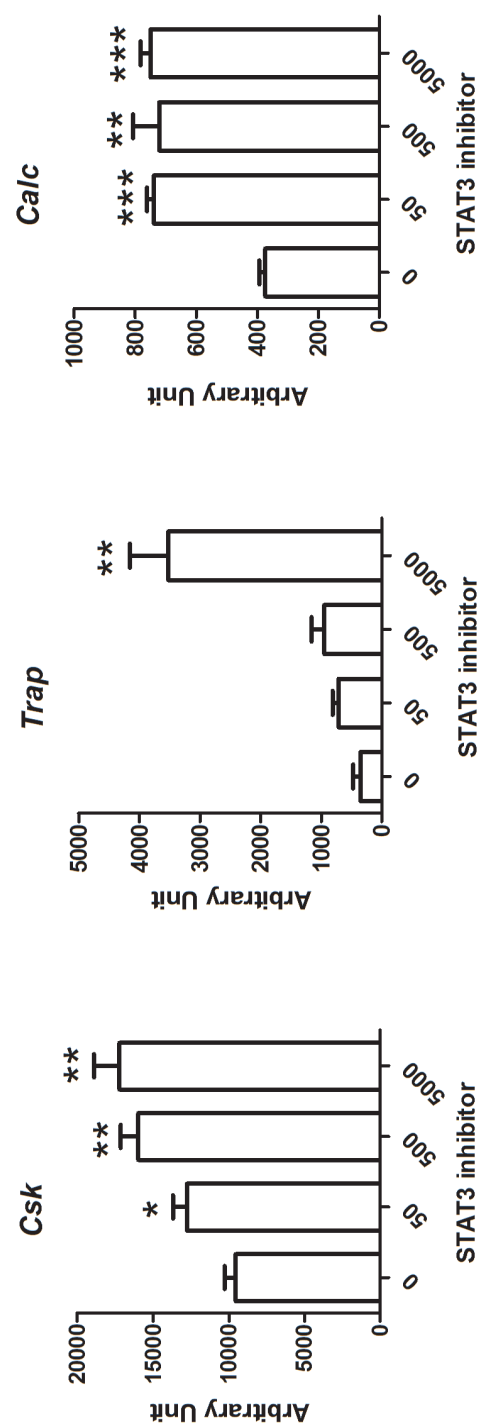


Figure 16. RANKL-induced osteoclast specific gene expression in the presence of a STAT3 inhibitor. BMDM were stimulated with 50 ng/mL RANKL for 4 days in the presence of increasing concentrations of the STAT3 SH2 domain inhibitor. Total RNA was isolated, converted to cDNA, and expression of *Apc5* (Trap), *Ctsk* (CSK), and *Calcr* (Calc) were analyzed by qPCR. Data are mean \pm s.e.m., * $p < 0.05$, ** $p < 0.01$, *** $p < 0.001$ analyzed using a student's T-test. Data are represented as arbitrary units relative to 18s rRNA.

Figure 16. RANKL induced osteoclast-specific gene expression of murine bone-marrow derived macrophages in the presence of a STAT3 inhibitor

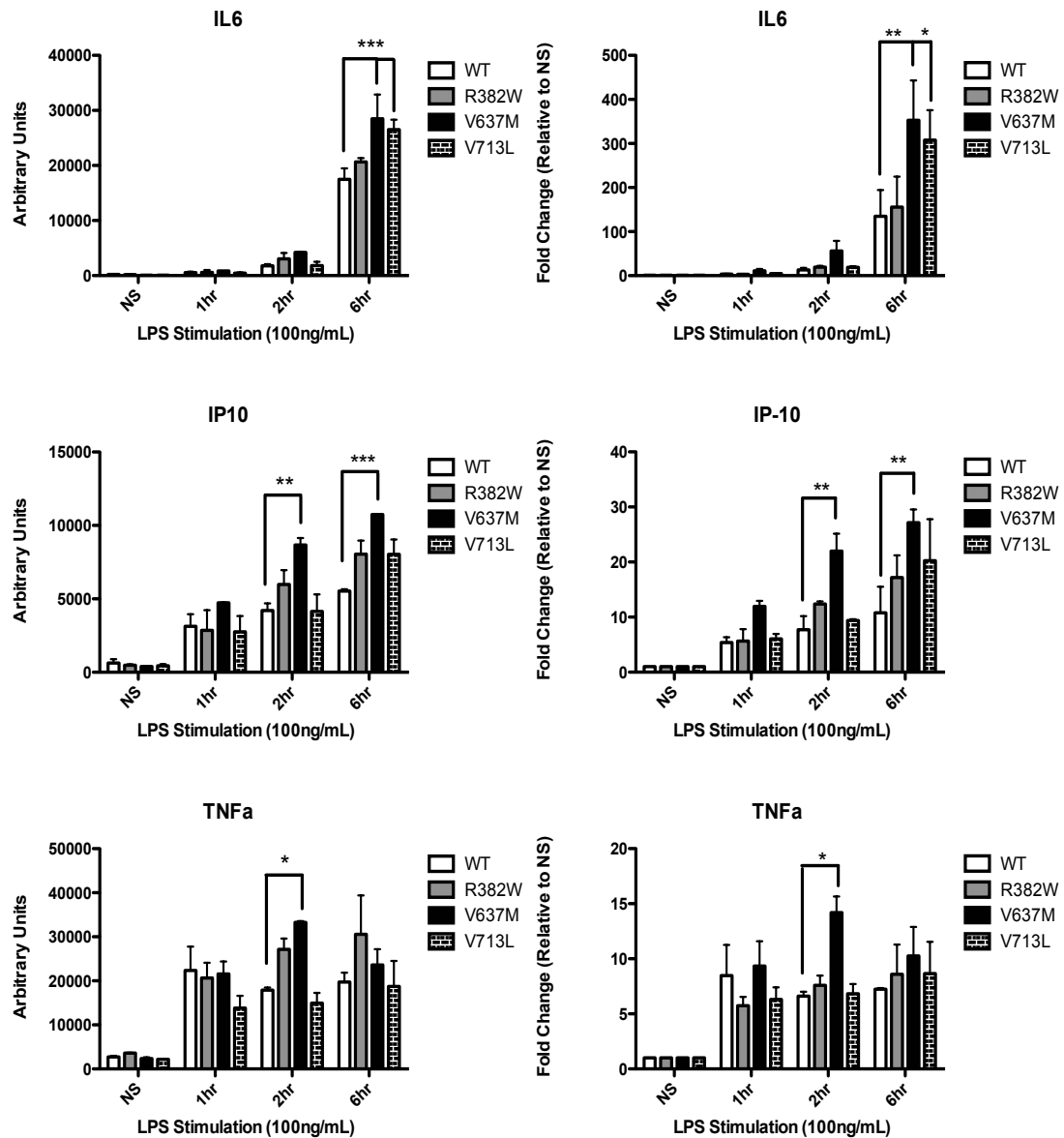


deregulate this pathway, we examined LPS-responsive gene expression. LPS is a known ligand for TLR4. Activation of TLR4 by LPS also induces the activation of NFκB [23][24][26]. Thus, we overexpressed the HIES mutant constructs in the mouse macrophage cell line, RAW, and examined LPS-responsive gene expression.

After confirmation of the expression of the STAT3 HIES mutants in RAW cells (Fig. 8), we stimulated the cells with LPS 0, 1, 2 or 6 hours and assayed the expression of inflammatory genes known as NFκB targets, including *Il6*, *Tnf* (TNFα), and *Cxcl10* (IP-10) (Fig. 17). We found in cells overexpressing WT STAT3 that *Il6* expression peaked at 6 hours post-stimulation with an approximate 200-fold induction relative to unstimulated cells. *Cxcl10* mRNA also peaked with similar kinetics with an approximate 15-fold increase in expression relative to unstimulated cells. *Tnf* mRNA expression appeared much earlier, at 1 hour, and remained at similar levels throughout the time-course. In addition, *Tnf* mRNA had the lowest fold induction of the three genes (2x increase) compared to unstimulated cells. RAW cells overexpressing the STAT3 V637M mutant showed significantly higher expression of *Il6* at 6 hours both in relative expression ($p<.001$) and fold induction ($p<.01$) (Fig. 17, upper left and right panels, respectively), compared to cells expressing WT STAT3. This *Il6* expression reached as high as a 400-fold increase relative to unstimulated cells, almost twice what WT STAT3 was found to induce. The V637M mutant displayed similar kinetics of *IL6* expression to WT STAT3. Cells expressing this mutant displayed comparable mRNA expression levels and kinetics for *Cxcl10* and *Tnf*, although the kinetics of *Tnf* expression were slightly different with the expression peaking at 2 hours versus WT which peaked at 1 hour. Cells expressing the V713L mutant displayed significantly higher IL-6 expression, similar to the V637M mutation, again reaching almost twice the induction of WT. However, statistical significance was not obtained with either *Cxcl10*

Figure 17. LPS-induced inflammatory gene expression in RAW cells overexpressing the STAT3 HIES mutants. RAW cells expressing the various STAT3 HIES mutants were unstimulated or stimulated with 100 ng/mL LPS for 1, 2 or 6 hours and then total RNA was extracted. cDNA was prepared and analyzed for expression of *IL6*, *Cxcl10* (IP-10), and *Tnf* by qPCR. Data are mean \pm s.e.m., * $p < 0.05$, ** $p < 0.01$, *** $p < 0.001$ analyzed by a 2-way ANOVA and a Bonferroni post-test. Data is represented as arbitrary units relative to 18s rRNA and fold change normalized to unstimulated cells for each mutant.

Figure 17. LPS-induced inflammatory gene expression in RAW cells overexpressing the STAT3 HIES mutants



or *Tnf* mRNA expression. Interestingly, while overexpressing STAT3 with the R382W mutation resulted in slightly higher levels of all three genes, in no case was this significant. Thus the HIES mutations we investigated lead to enhanced NFκB-mediated inflammatory gene expression in macrophages following TLR4 activation, which suggests that STAT3 function may be important for restraining this gene expression.

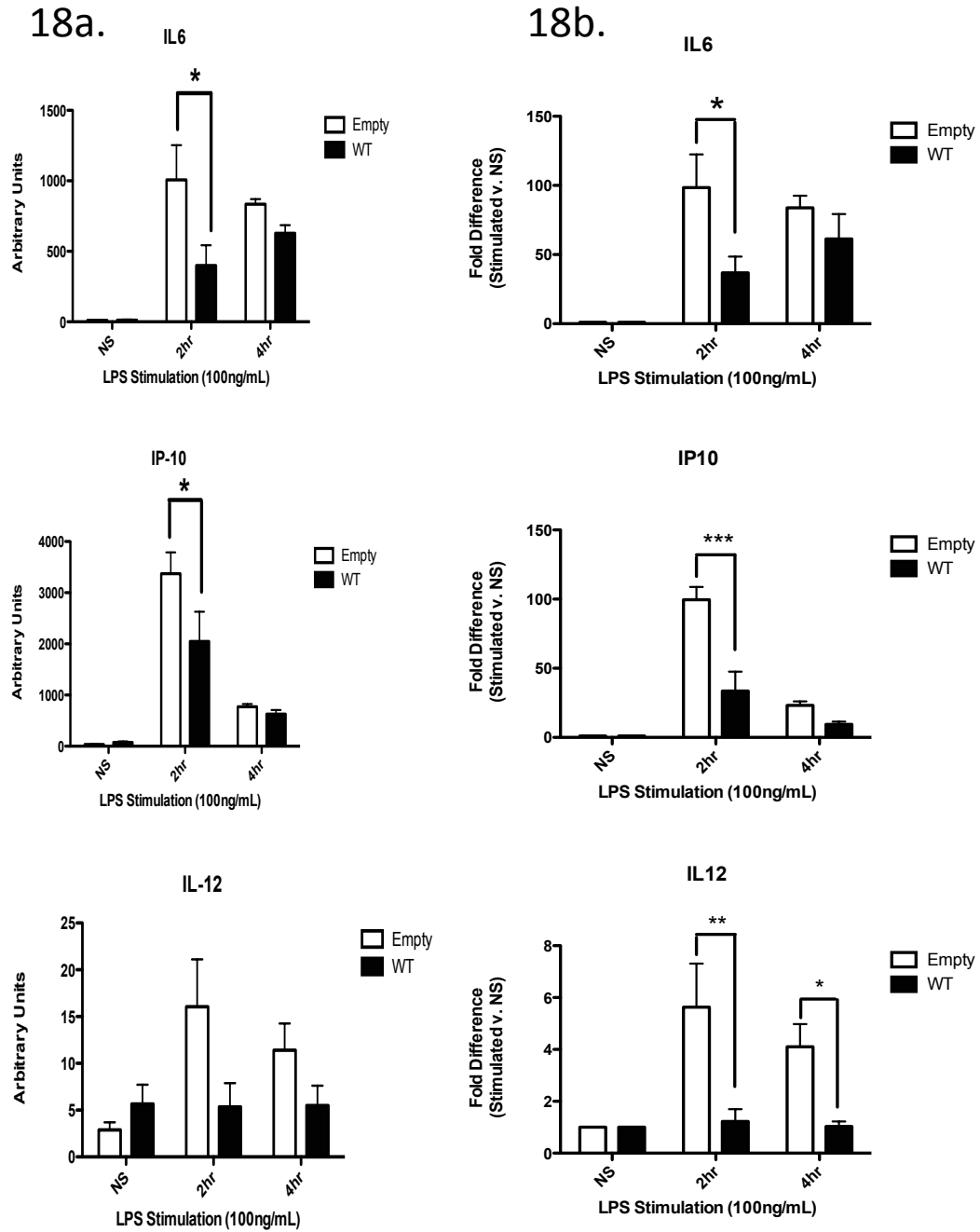
Analysis of the LPS-induced inflammatory gene expression in mouse embryonic fibroblasts overexpressing STAT3

While it is evident that STAT3 negatively regulates NFκB-mediated inflammatory gene expression in macrophages, and that the domains thought to be important for transcriptional function participate in this regulation, we were interested in whether STAT3 also participates in a similar manner in non-hematopoietic tissues. This would establish STAT3 as a more global regulator of inflammatory gene expression. To evaluate this possibility, we used a STAT3-deficient MEF cell line and reconstituted with WT STAT3 or GFP-empty vector (Fig. 10) as a reference for gene expression in the absence of STAT3 and to control for the effect the infection may have had on this gene expression.

To examine the effect of STAT3 on NFκB-mediated inflammatory gene expression in fibroblasts, we stimulated the MEFs expressing either WT STAT3 or GFP-empty vector with LPS and then assayed expression of NFκB inflammatory gene targets via qPCR (Fig. 18). We found a markedly decreased expression of *Il6*, *Cxcl10*, and *Il12* mRNA after WT STAT3 overexpression compared to the GFP-empty transduced STAT3-deficient cells. The relative expression levels of *Il6* and *Cxcl10* became significantly less in WT cells than GFP-empty at 2 hours ($p < .05$) (Fig. 18a),

Figure 18. LPS-induced inflammatory gene expression in STAT3-deficient MEFs overexpressing WT STAT3. STAT3-deficient MEFs stably expressing either a GFP-empty vector or WT STAT3 were unstimulated or stimulated with 100 ng/mL LPS for 2, or 4 hours and then total RNA was extracted. The mRNA was reverse transcribed to cDNA which was then analyzed for *IL6*, *Cxcl10* (IP-10), and *IL12* by qPCR. (a) Data are represented as arbitrary units relative to 18s rRNA. (b) Data are represented as fold change relative to the unstimulated sample. Data are mean \pm s.e.m., * $p < 0.05$, ** $p < 0.01$, *** $p < 0.001$ analyzed by 2-way ANOVA and Bonferroni post-test.

Figure 18. LPS-induced inflammatory gene expression in STAT3-deficient MEFs overexpressing WT STAT3



and a similar result was obtained when examining the fold change (Fig. 18b). *IL6*, *Cxcl10* and *IL12* were also significantly induced in GFP-empty transduced cells compared cells expressing WT STAT3 (Fig. 18b). When WT STAT3 was absent, *IL6* and *Cxcl10* expression were induced 2 fold more than when STAT3 was present. *IL12* was induced up to 7 fold when similarly compared.

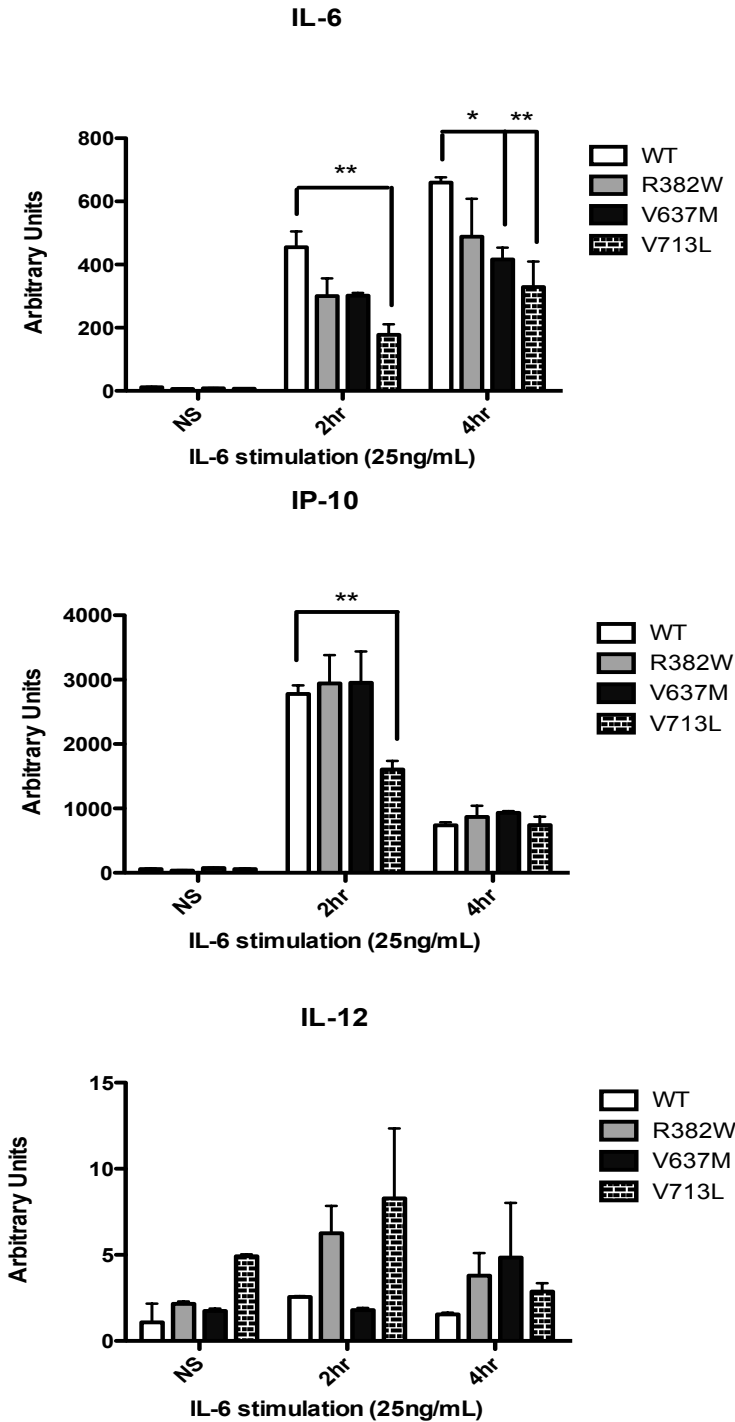
Interestingly, the forced expression of STAT3 also changed the kinetics of the expression for both *IL6* and *IL12*. *IL6* mRNA expression peaked at 2 hours in cells expressing GFP-empty vector whereas the WT STAT3 overexpressing cells exhibited delayed induction peaking at 4 hours (Fig. 18a). Significantly, *IL12* showed no induction when STAT3 was present and was 7 fold less than empty-vector transduced STAT3-deficient cells (Fig. 18b). Thus, in non-hematopoietic tissues, STAT3 functions similarly as in immune cells by inhibiting LPS-induced NFkB-mediated inflammatory gene expression.

The effect of HIES mutants on LPS-induced inflammatory gene expression in STAT3-deficient MEFs

Our results showed that overexpression of STAT3 HIES mutants resulted in increased inflammatory gene expression in macrophages (Fig. 17), and that STAT3 overexpression in STAT3-deficient MEFs dampened inflammatory gene expression (Figs. 18a & 18b), indicating STAT3 negatively regulates inflammatory gene expression in both systems. Thus, we sought to examine the affect of these mutants on inflammatory gene expression in STAT3-deficient MEFs. We stimulated MEFs that stably express the HIES mutants with LPS for 2 or 4 hours and assayed for *IL6*, *Cxcl10*, and *IL12* mRNA expression by qPCR. Surprisingly, we found no increase in either *IL6* or *Cxcl10* expression at either time point (Fig. 19). We did observe increased

Figure 19. LPS-induced inflammatory gene expression in STAT3-deficient MEFs expressing the STAT3 HIES mutants. STAT3-deficient MEFs stably expressing WT STAT3 or the STAT3 HIES mutants were unstimulated or stimulated with 100 ng/mL LPS for 2 or 4 hours and then total RNA was extracted. cDNA was generated and analyzed for expression of *IL6*, *Cxcl10* (IP-10), and *IL12* by qPCR. Data are represented as arbitrary units relative to 18s rRNA. Data are mean \pm s.e.m., * $p < 0.05$, ** $p < 0.01$, analyzed by a 2-way ANOVA and Bonferroni post-test.

Figure 19. LPS-induced inflammatory gene expression in STAT3-deficient MEFs overexpressing the STAT3 HIES mutants



Ii12 gene expression levels in cells expressing the HIES mutants compared to cells expressing WT STAT3, however they were determined to be statistically insignificant. *Ii6* showed significantly lower expression in cells with the V637M and V713L mutants in comparison to cells with WT STAT3. *Cxcl10* showed significantly lower expression only in the V713L mutant cells. Thus, expressing the HIES mutants in MEFs lacking endogenous STAT3 does not enhance their expression of LPS-induced inflammatory gene compared to WT STAT3 as was initially hypothesized.

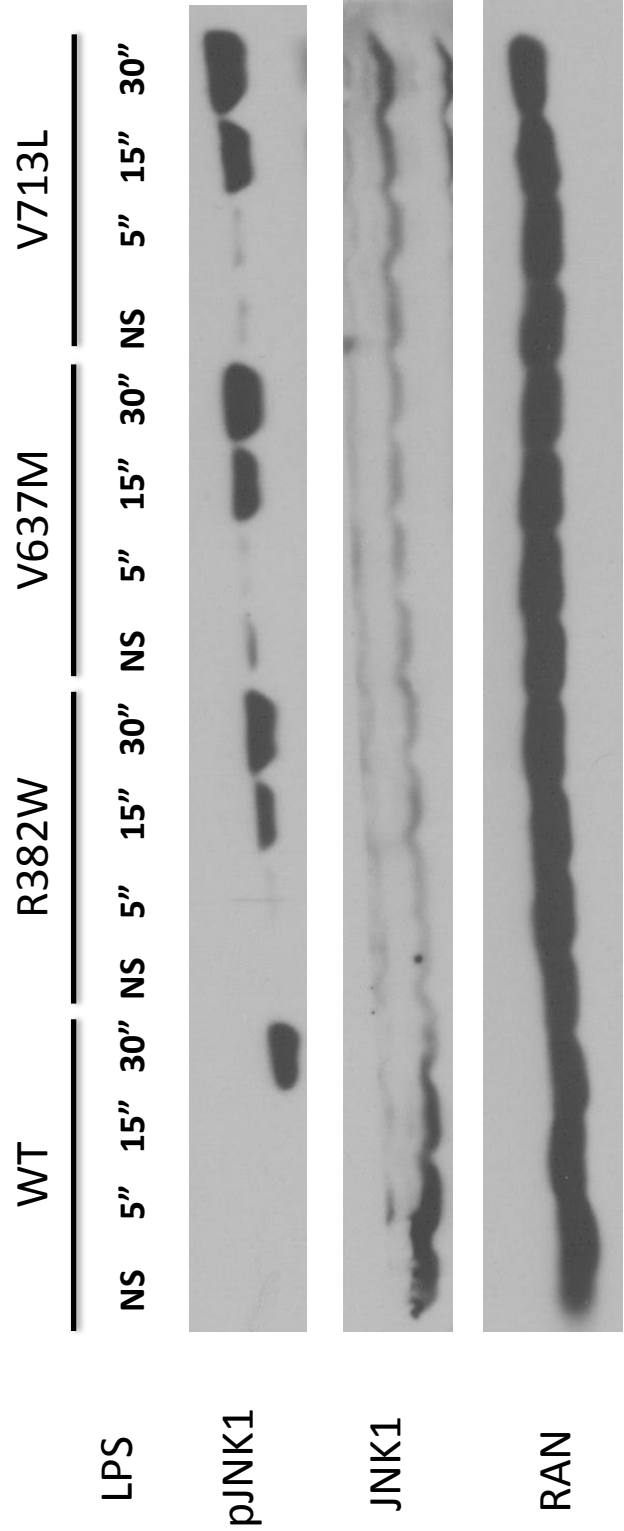
Examination of mitogen activated protein kinase (MAPK) signaling after LPS stimulation in macrophages expressing the HIES mutants

Both the cytokine profile we observed with the HIES STAT3 point mutations in murine macrophages (Fig. 17), and the cytokines found in the blood of patients with HIES [84][89], indicate a possible role for involvement of both NFκB and MAPK signaling in hematopoietic cells. *Ii6* and *Cxcl10* are regulated by both NFκB and AP-1 binding in their promoters [109][110] and *Tnf* expression has also been linked to both NFκB and AP-1 activation [111]. In addition, in B-cells, NFκB regulates AP-1 activation after LPS stimulation [112]. Therefore, we hypothesized that the enhanced inflammatory gene expression in RAW cells could be due to the activation of both signaling pathways.

Using the RAW cells overexpressing either WT STAT3 or STAT3 HIES mutants, we stimulated them with LPS for 5, 15, or 30 minutes and then analyzed phosphorylation of c-Jun N-terminal Kinase 1 (JNK1) by immunoblot (Fig. 20). JNK1 is downstream of TAK1 but upstream of AP-1 in the MAPK pathway [113][114]. JNK1 becomes activated after tyrosine phosphorylation [114]. In cells overexpressing WT STAT3, we found that JNK was activated by 30 minutes post-stimulation. Conversely,

Figure 20. LPS-induced JNK1 activation in RAW cells expressing the STAT3 HIES mutants. The RAW cells stably expressing the STAT3 HIES mutants were unstimulated or stimulated with 100 ng/mL LPS for 5, 15, or 30 minutes and then whole cell lysates were isolated and analyzed by western blot for tyrosine phosphorylated JNK1 and total JNK1 expression. RAN was used as a loading control.

Figure 20. LPS-induced JNK1 phosphorylation in RAW cells overexpressing the STAT3 HIES mutants



when any of the HIES mutants were overexpressed, pJNK1 levels appeared as early as 5 minutes with significantly higher expression, compared to macrophages expressing WT STAT3, as stimulation time increased to 15 and 30 minutes.

Our preliminary data examining whether the STAT3 HIES mutants affect NFκB activation, using analysis of phosphorylated-IκBα and degradation of IκBα, indicates a possible enhancement of NFκB activation as well but further confirmation is required (data not shown). Thus, our results suggest that loss of STAT3 function leads to enhanced MAPK signaling, which may be partially responsible for the increased inflammatory gene expression we observe in the macrophages expressing the HIES STAT3 mutants. Our preliminary results also indicate a possible increase in NFκB signaling in the presence of STAT3 HIES mutant overexpression.

Discussion

STAT3 is an important molecule in many diverse and distinct cellular processes including survival, proliferation, differentiation, inflammation and oncogenesis [36][41][43][67][76][77]. Traditionally STAT3 has been described as a transcription factor, similar to the other STAT family members [45]. New evidence suggests that this may be an oversimplified view of the ways STAT3 functions within a cell [61][62][63]. Previous studies have described an anti-inflammatory role for STAT3 through participation in and regulation of IL-10 signaling [69][70]. In this project, we examine another mechanism whereby STAT3 may negatively regulate inflammation and differentiation, via crosstalk with the NFκB signaling pathway. We sought to better understand how this regulation occurs, and to gain more insight into how the mutations in HIES lead to enhanced inflammatory gene expression.

Previous studies have identified various mutations in the STAT3 gene in humans diagnosed with Hyper-IgE syndrome [88][89]. The majority of these are point mutations with several deletions also identified. Interestingly, all of these mutations were found in domains thought to be important for STAT3 transcriptional activity [53][54]. To examine how the different domains affect STAT3's regulation of NFκB-mediated gene expression, we chose to analyze three of these point mutations, one in each different domain (DNA-binding, SH2, TAD) (Fig. 6).

To understand the mechanism by which these mutants were affecting the function of STAT3, we first had to analyze their activation potential. Previous studies have suggested that STAT3 containing a mutation in the DNA-binding domain (R382W) can be tyrosine phosphorylated whereas STAT3 containing a mutation found in the SH2 domain (V637M) cannot be [98]. These studies were conducted in COS-7 cells, which express a low level of endogenous STAT3 [55], transiently transfected with either STAT3 mutant construct after EGF stimulation, therefore we wanted to confirm this observation in cells stably expressing the HIES mutants without any confounding endogenous STAT3.

Using STAT3-deficient MEFs expressing the STAT3 HIES mutants, we confirmed the previous observation that the R382W mutant can be tyrosine phosphorylated [98] (Fig. 11). We also observed slightly higher amounts of tyrosine phosphorylation of the R382W mutant than that in WT STAT3 expressing cells despite similar total STAT3 levels (Fig. 11). We also observed this enhanced tyrosine phosphorylation when we examined total STAT3 activation in RAW cells expressing the STAT3 HIES mutants (Fig. 9a). This may indicate a mechanism that fails to attenuate the cytokine signal leading to prolonged phosphorylation. One explanation could be the lack of SOCS3 (Fig. 14) due to the loss of the R382W mutant's

transcriptional activity (Fig. 12). SOCS3 has been shown to be an important inhibitor of cytokine signaling, especially after IL-6 stimulation *in vivo* [72]. We also confirmed the previous observation that the V637M mutation completely prevents STAT3 from becoming tyrosine phosphorylated [98]. We hypothesize the mutation may somehow prevent STAT3 binding the phosphotyrosine on gp130, similarly to how the STAT3 inhibitor leads to diminished STAT3 tyrosine phosphorylation after G-CSF stimulation (Fig. 15a). However, further analysis is required to confirm that this mutation physically prevents STAT3's association with the phosphotyrosine on gp130 or by some other unknown mechanism. Since the identification of the mutation in the TAD (V713L) has been established [98], no research has been focused on determining how this mutation alters STAT3 function to result in the HIES phenotype. To our knowledge we are the first to show that the V713L mutation does not completely block STAT3's ability to become tyrosine phosphorylated (Fig. 11). However, STAT3 containing this mutation becomes phosphorylated less efficiently than either WT STAT3 or STAT3 with the R382W mutation. Interestingly, and in accordance with this modest phosphorylation, we also showed this mutant has a low level of transcriptional ability (Fig. 12), which would make it difficult to ascribe dominant negative ability to this mutant, at least in terms of severely blocking WT STAT3's transcriptional function.

In order for a protein to be considered dominant negative, it must interfere with the function of the WT protein often exhibiting a phenotype more severe than the loss of only a single allele [115]. To determine whether each of the STAT3 HIES mutants was dominant negative, we overexpressed these mutants in a murine macrophage cell line (RAW), which expresses endogenous STAT3 (Fig. 9b). We sought to examine whether these mutants affected total STAT3 phosphorylation in the presence of endogenous STAT3. We again observed an enhanced tyrosine phosphorylation with

the R382W mutant and moderately less tyrosine phosphorylated STAT3 in the V713L expressing cells (Fig. 9a). The data from the STAT3-deficient MEFs after IL-6 stimulation indicates the V637M mutant has a complete defect in tyrosine phosphorylation (Fig. 11). Therefore, we conclude that the phosphorylated STAT3 observed in the RAW cells expressing the V637M STAT3 mutant (Fig. 9a) is solely the endogenous STAT3. Additionally, this phosphorylation level is similar to the level found in uninfected RAW cells (Fig. 9b). Unfortunately, due to the intrinsic tyrosine phosphorylation of the R382W and V713L mutants, it was difficult to conclude whether they abrogated phosphorylation of endogenous STAT3. We may be able to infer their effect, however, based on what we know about the location of each mutation. The R382W mutation is located in the DNA-binding domain and has no effect on the intrinsic tyrosine phosphorylation of STAT3; therefore we could hypothesize that this mutant would have no inhibitory effect on phosphorylation of endogenous STAT3. The V637M mutation is in the SH2 domain and therefore completely prevents tyrosine phosphorylation of STAT3, presumably due to a defect in the interaction at the receptor. This also should not affect endogenous STAT3 phosphorylation because the phosphorylation occurs with the monomeric STAT3. For the same reason, we can hypothesize the V713L mutant would not affect endogenous STAT3 phosphorylation. So the question remained, if these mutations are not affecting the phosphorylation of WT STAT3, do they truly exert dominant negative activity and if so, how is this accomplished?

The initial paper describing the STAT3 mutations within the DNA-binding domain in patients with HIES tested the dominant negative activity of the R382W mutant through analysis of its effect on the ability of WT STAT3 to initiate transcription of a STAT3 reporter [88]. In this study, Minegishi et al analyzed the dominant negative

activity in cells expressing a low level of endogenous STAT3 [116] and did not report the ratio of WT STAT3 to mutant STAT3 required for inhibition. Therefore, we sought not only to confirm the dominant negative activity of the R382W mutant and determine the potency by which it accomplishes this activity, but also examine the dominant negative activity of the V637M and V713L mutants. We chose to use the STAT3-deficient MEF cell line to eliminate the confounding effect of endogenous STAT3 and more accurately determine the amount of mutant protein needed to inhibit WT STAT3 activity. As expected, we found that the R382W STAT3 mutant inhibited WT STAT3's ability to initiate transcription of a STAT3 luciferase reporter; however this inhibition required four times as much mutant protein to obtain statistical significance (Fig. 13).

The V637M mutant, which failed to be phosphorylated and most likely failed to inhibit phosphorylation of endogenous STAT3, also failed to inhibit WT STAT3's transcriptional function as judged by the reporter assay. In contrast, macrophages stably expressing this mutant exhibited significantly reduced *Socs3* gene expression (Fig. 14). This is indicative of the V637M mutant protein interfering with endogenous WT STAT3 function [101][102]. The disagreement between these two sets of data could be a technical issue given the amount of mutant needed to elicit any inhibition in the luciferase assays (4:1 at the least), or it could indicate that the reduction in *Socs3* gene expression is due to a mechanism independent of directly blocking transcription. Interestingly, the V713L mutation exhibits a trend toward dominant negative activity over WT STAT3's transcriptional function (Fig. 13) as low as a 4:1 WT to mutant ratio with significance arising at 1:10. However, while the level of *Socs3* is diminished compared to WT, the change is insignificant and nowhere near the level observed with the R382W and V637M mutants (Fig. 14). This may be due in part to the inherent transcriptional ability of this mutant on its own (Fig. 12).

The only mutation for which any direct mechanism has been elucidated is the R382W mutation, which was shown to completely abrogate the DNA-binding ability of STAT3 to the *Socs3* promoter [117]. Our *Socs3* gene expression results in both macrophages and MEFs, and our reporter assay results with this mutation, correlate well with this data. On the other hand, no evidence has been provided regarding the mechanism by which the other two mutants, V637M and V713L, functionally inhibit STAT3 activity. Our data confirm the total lack of phosphorylation of the V637M mutant [98] but show that it most likely does not affect endogenous WT STAT3 phosphorylation or direct transcriptional function. However this mutant still interferes with WT STAT3's function as shown through the reduced *Socs3* expression in RAW cells expressing this mutant. Initially, we hypothesized that in the HIES patient setting, the reduction in WT STAT3 activity in the presence of the V637M mutant allele could be due to an overall reduction in available WT STAT3 within the cell. This is due to the fact that ideally at a 1:1 WT to mutant ratio, the presence of this mutant would reduce the amount of transcriptionally active WT STAT3 by 50%. Due to the importance of STAT3 in many cellular processes [36][42][43][52] and the conclusion that this mutation is responsible for the HIES phenotype in several individuals [89], this hypothesis seems plausible. However, given that mice lacking one full WT STAT3 allele show no adverse effects and do not present with an HIES phenotype [52], this may not be the explanation. However it is possible this mutation does block the ability of WT STAT3 to initiate transcription but due to technical difficulties or the sensitivity of our luciferase assay we were unable to detect it. To confirm this hypothesis would require further study.

As we showed, the V713L mutation doesn't fully inhibit phosphorylation of STAT3, thus it has a minimal amount of transcriptional activity. Even so, it significantly

reduced WT STAT3's ability to transcribe the luciferase gene in our reporter assays and marginally reduced SOCS3 expression in RAW cells. We believe this lends evidence to our hypothesis that this mutation, by participating in the formation of the SH2 domain, may lead to unstable interactions either at the receptor or once dimerized. This could lead to attenuated dimerization once phosphorylated or once bound to promoters. Further elucidation of this mechanism would require either co-immunoprecipitations with the receptor or *in vitro* binding assays. It is also possible that this mutation changes the conformation of the TAD such that it is no longer able to enhance transcription [55].

Now that we have a little better idea of how these mutants function, we sought to utilize them to determine how STAT3 may be interacting with the NFκB signaling pathway resulting in the phenotypes observed in patients with HIES and mice lacking hematopoietic STAT3 (Table 1). We chose to focus primarily on the increased osteoporosis and inflammation. The cytokine profile we examined was based on previous reports regarding known NFκB and AP-1 targets, namely *Il6*, *Cxcl10* (IP-10), *Tnf* (TNFα), and *Il12* [78][109][110][111][118][119]. As figures 1 and 2 depict, the RANKL and LPS pathways share several common elements upstream of the most striking similarity, NFκB activation. Both pathways use TRAF6 at early stages to lead to the activation of TAK1 [8][22][120]. TAK1 is a common signaling component between the NFκB and MAPK pathways. This corroborates the data showing that the majority of the inflammatory cytokines enhanced in HIES are targets of the terminal transcription factors of these two pathways (NFκB and AP-1) [114-116]. Due to the deregulation of both of these pathways in patients with HIES and mice lacking STAT3 in the hematopoietic system [66][67][84][89][121](Table1), we hypothesized that STAT3 might act to negatively regulates both pathways through a common signaling

component, however confirming this was out of the scope of the current project. We chose to focus on whether STAT3 was negatively regulating these pathways via a transcriptional mechanism or an alternative method.

Our data indicated an importance for the SH2 domain in regulating osteoclastogenesis through the use of an antagonistic inhibitor for this domain (Fig. 16). Due to difficulties in differentiating the RAW cells, in addition to technical issues infecting primary murine macrophages, we were unable to verify the involvement of the other domains using the STAT3 HIES mutants. However, we can establish a tenuous indirect importance of the DNA-binding and SH2 domains due to the presence of osteoclastogenesis deregulation in patients carrying mutations in these domains [89][98].

With regards to the enhanced inflammatory gene expression seen in both human patients and hematopoietic STAT3-deficient mice, we have clearly indicated a function for the DNA-binding domain, SH2 domain, and TAD in this regulation. In all three cases, we saw increased mRNA expression of *Il6*, *Cxcl10*, *Tnf* compared to WT STAT3. Even in non-hematopoietic tissues, such as MEFs, we have shown that STAT3 expression significantly reduced the mRNA expression of *Il6*, *Cxcl10*, *Il12* (Fig. 18). However, in non-hematopoietic cells, the HIES mutants may not be acting as they do in the macrophages because we see a significant reduction in expression of these genes after LPS stimulation (Fig. 19) which is in stark contrast to our data comparing GFP-empty vector transduced cells with WT STAT3 transduced cells (Fig. 18). This may indicate that MEFs are not a good system for our analysis or, more likely that the mechanism we hypothesize that is leading to increase inflammatory gene expression, is not active in non-hematopoietic cells.

Next we wanted to further examine the developing relationship between STAT3 and NFκB. To this point, we had only shown indirectly that loss of STAT3 function, by mutation or exogenous inhibition of the DNA-binding domain, SH2 domain, or TAD leads to increased gene expression of inflammatory mediators, which are NFκB and AP-1 targets, and enhanced osteoclastogenesis, a process that is NFκB-dependent. Therefore, we intended to examine whether the loss of STAT3 function led to increased NFκB activation. Preliminary results examining phosphorylation of the inhibitor of NFκB, IκBα, showed enhanced phosphorylation as well as enhanced degradation (data not shown), which follows this phosphorylation [122]. We examined the phosphorylation of JNK1, which is part of the MAPK pathway downstream of TAK1 activation and serves to activate the AP-1 family of transcription factors [113][114]. Cells expressing the HIES mutants began activating JNK1 as early as 5 minutes post-stimulation (Fig. 20), which was significant because cells expressing WT STAT3 did not exhibit JNK phosphorylation until 30 minutes post-LPS stimulation. This suggests that MAPK signaling, induced by TLR4 activation of macrophages, is negatively regulated by STAT3 and most likely deregulated in patients with HIES.

In this study, we have shown that STAT3 negatively regulates NFκB and MAPK-mediated inflammatory gene expression in both macrophages and non-hematopoietic fibroblasts. In addition, we found that STAT3 inhibits the expression of genes specific for osteoclastogenesis, a process that is NFκB dependent. We have shown that the SH2 domain is required for this regulation and that the DNA binding domain and the TAD are also involved in regulating the inflammatory gene expression. From our analysis of the point mutations identified in patients with HIES, we have confirmed previous reports regarding the activation capabilities of STAT3 when mutations occur in the DNA-binding and SH2 domains and we were the first to show

that the V713L mutation doesn't completely block STAT3 phosphorylation or transcriptional function. We demonstrated that the R382W, V637M, and V713L mutants elicit dominant negative activity either through reduction of luciferase reporter transcription or endogenous *Socs3* expression. Data regarding the V637M mutant disagreed, raising several questions regarding how this mutation leads to the inflammatory and bone phenotypes observed in HIES. We have developed several alternative hypotheses, which will allow us to pursue answers to these questions in future studies.

In one model, the V637M mutation could reduce the amount of global STAT3 signals within the cell, which would be significant, as it would show what even a slight loss in STAT3 signaling could lead to. However in light of data in mice heterozygous for *Stat3* [52], this seems unlikely. Another possibility came out of the evidence that this mutant STAT3 protein cannot be phosphorylated. Several groups have identified roles for unphosphorylated STAT3 (U-STAT3), which could offer alternative explanations for the observations obtained in this study regarding the V637M mutation. U-STAT3 has been shown to bind NF κ B after IL-6 stimulation and lead to its activation by displacement of I κ B α [68]. Another group identified a role for the *Drosophila melanogaster* STAT protein in maintaining heterochromatin stability [61] while a role was also identified for STAT4 and STAT6 in epigenetic modifications [64]. These observations could indicate that it is possible unphosphorylated STAT3 could regulate heterochromatin in such a way that it remains closed to the transcription of NF κ B-inhibiting proteins. However, we have to be careful to not overanalyze our data as this mutation could also function only to block binding and activation at the receptor but not to activated STAT3 monomers, something that has not been investigated.

Our data indicates a role for STAT3 in regulating NFκB and MAPK signaling via its intrinsic transcriptional activity, and highlights the necessity for two fully functional STAT3 alleles. However there are gaps that need to be filled prior to drawing any further, definitive conclusions. To extend this work, we intend to determine what STAT3's transcriptional target is and which protein in the NFκB pathway it is acting to repress. Secondly, we would like to determine the mechanism by which the V637M mutation is affecting STAT3's regulation of NFκB signaling. Since STAT3 monomers carrying this mutation cannot be phosphorylated, presumably they cannot bind phosphorylated STAT3 monomers. This indicates that only WT STAT3 monomers would be involved in the signaling. Thus the defect seen in our system as well as patients with this mutation remains to be determined, but could either be due to the reduction in activatable STAT3 or an unknown mechanism for unphosphorylated STAT3. Finally, we intend to confirm whether the V713L mutation destabilizes STAT3. Does the instability affect binding at the receptor, the promoter, or somewhere in between? Could it be due to some other reason, such as a conformational changes shielding the tyrosine residue from the receptor associated JAKs or phosphorylation of the serine residue located with this domain?

Regardless of the several questions which this study raises, we have extended knowledge of the mechanism leading to enhanced inflammation and osteoporosis in patients with HIES. We have also established STAT3 as a negative regulator of NFκB- and MAPK- induced inflammatory gene expression and MAPK activation.

Figure 21. Schematic diagram of our working model for the interplay between STAT3 and NFκB/MAPK. Diagram representing WT STAT3 negatively regulating NFκB/MAPK leading to repressed inflammatory and osteoclast-specific gene expression. NFκB and MAPK signaling gets activated which leads to expression of STAT3-activating signals. These lead to STAT3 aiding in the transcription of a gene which goes on to repress proteins upstream of TAK1 thereby inhibiting further NFκB and MAPK activation. Dotted arrows represent a diminished signal.

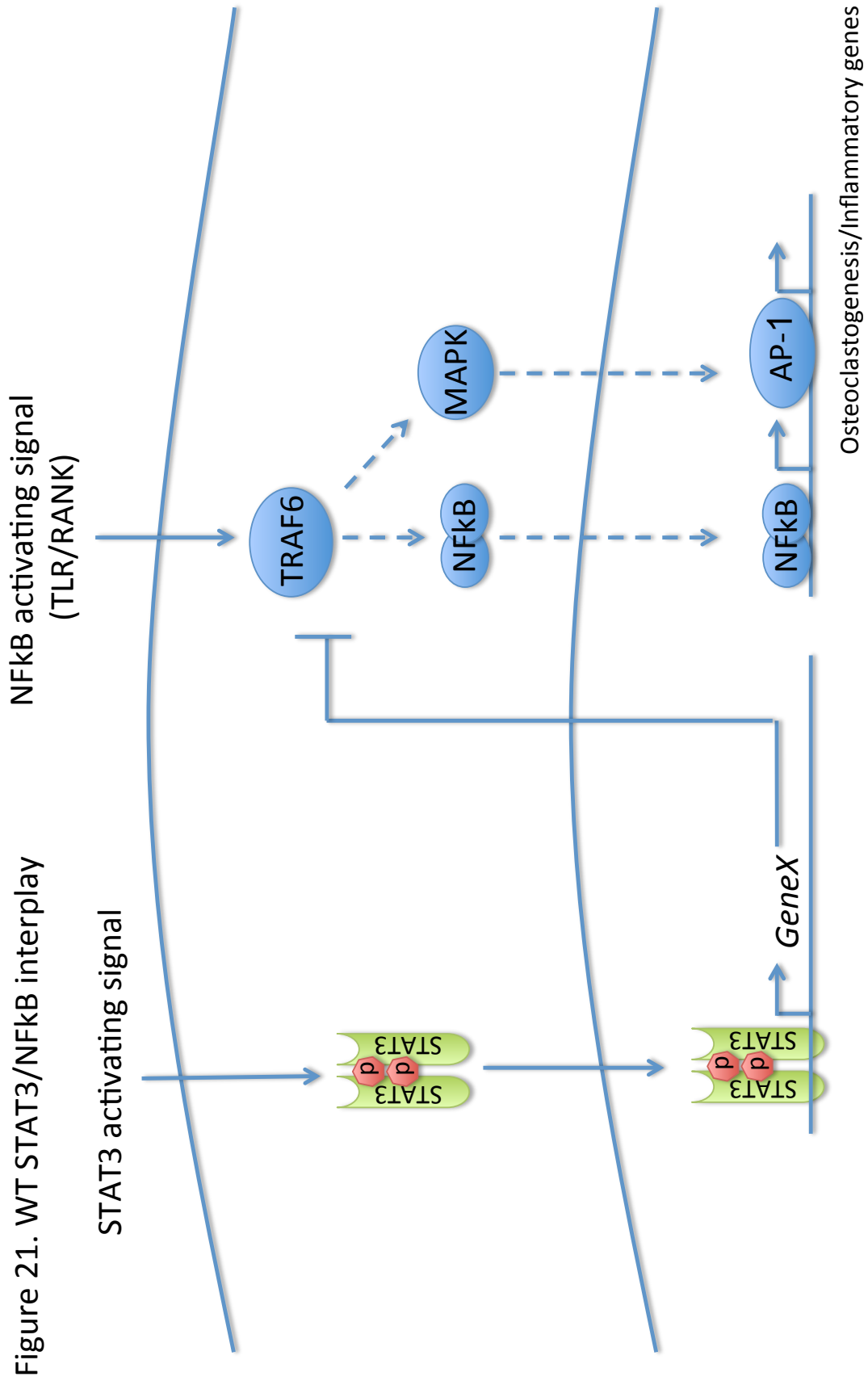
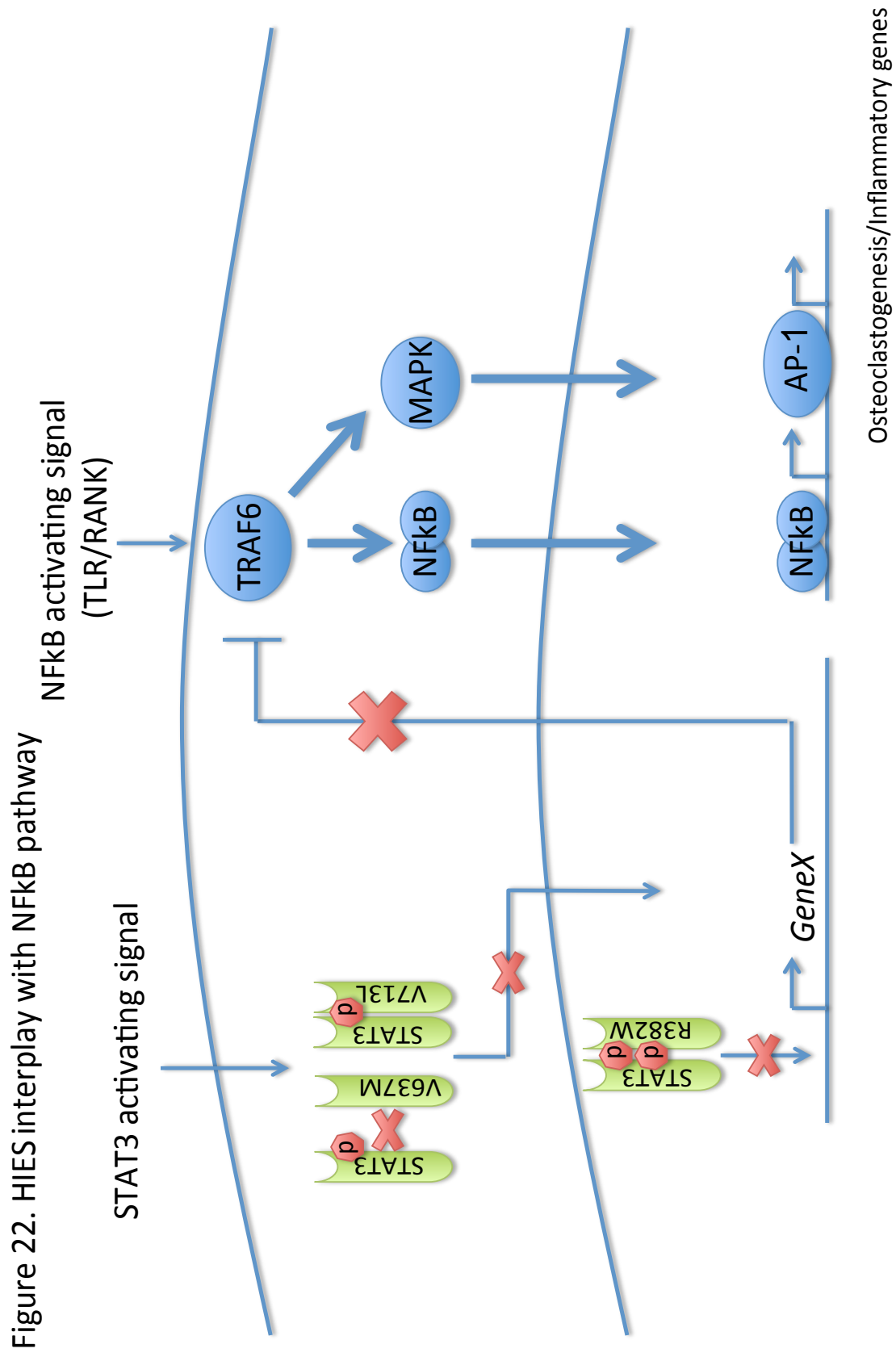



Figure 22. Diagram representing our working model with regards to how the HIES mutants affect the regulation seen in Figure 21. The HIES mutants interfere with STAT3's transcription of "gene x" thus enhancing NFkB-mediated gene transcription. The R382W mutant inhibits the ability to bind DNA, whereas the V637M mutant acts through an unknown mechanism, and the V713L mutation possibly destabilizes STAT3's dimerization or interaction at the receptor. Bolded arrows represent an enhanced signal.



References

- [1] E. Passegue, C. Jamieson, L. Ailles, I. Weissman, Normal and leukemic hematopoiesis: are leukemias a stem cell disorder or a reacquisition of stem cell characteristics?, *Proceedings of the National Academy of Sciences of the United States of America* 100 Suppl 1 (2003) 11842-11851.
- [2] H. Yasuda, N. Shima, N. Nakagawa. Osteoclast differentiation factor is a ligand for osteoprotegerin/osteoclastogenesis-inhibitory factor and is identical to TRANCE/RANKL, *Proceedings of the National Academy of Science* (1998).
- [3] K. Fuller, B. Wong, S. Fox, Y. Choi, , TRANCE is necessary and sufficient for osteoblast-mediated activation of bone resorption in osteoclasts, *The Journal of Experimental Medicine* (1998)
- [4] J. Li, I. Sarosi, X. Yan, S. Morony, C. Capparelli, H. Tan, S. McCabe, R. Elliott, S. Scully, G. Van, S. Kaufman, S. Juan, Y. Sun, J. Tarpley, L. Martin, K. Christensen, J. McCabe, P. Kostenuik, H. Hsu, F. Fletcher, C. Dunstan, D. Lacey, W. Boyle, RANK is the intrinsic hematopoietic cell surface receptor that controls osteoclastogenesis and regulation of bone mass and calcium metabolism, *Proceedings of the National Academy of Sciences of the United States of America* 97 (2000) 1566-1637.
- [5] H. Takayanagi, S. Kim, T. Koga, H. Nishina, M. Isshiki, H. Yoshida, A. Saiura, M. Isobe, T. Yokochi, J.-i. Inoue, E. Wagner, T. Mak, T. Kodama, T. Taniguchi, Induction and activation of the transcription factor NFATc1 (NFAT2) integrate RANKL signaling in terminal differentiation of osteoclasts, *Developmental cell* 3 (2002) 889-1790.
- [6] K. Saito, N. Ohara, H. Hotokezaka, S. Fukumoto, K. Yuasa, M. Naito, T. Fujiwara, K. Nakayama, Infection-induced up-regulation of the costimulatory

- molecule 4-1BB in osteoblastic cells and its inhibitory effect on M-CSF/RANKL-induced in vitro osteoclastogenesis, *The Journal of biological chemistry* 279 (2004) 13555-13618.
- [7] D. Anderson, E. Maraskovsky, W. Billingsley, W. Dougall, M. Tometsko, E. Roux, M. Teepe, R. DuBose, D. Cosman, L. Galibert, A homologue of the TNF receptor and its ligand enhance T-cell growth and dendritic-cell function, *Nature* 390 (1997) 175-184.
- [8] J. Mizukami, G. Takaesu, H. Akatsuka, H. Sakurai, J. Ninomiya-Tsuji, K. Matsumoto, N. Sakurai, Receptor Activator of NF- κ B Ligand (RANKL) Activates TAK1 Mitogen-Activated Protein Kinase Kinase Kinase through a Signaling Complex Containing RANK, TAB2, and TRAF6, *Molecular and Cellular Biology* 22 (2002).
- [9] L. Galibert, M. Tometsko, D. Anderson, D. Cosman, W. Dougall, The involvement of multiple tumor necrosis factor receptor (TNFR)-associated factors in the signaling mechanisms of receptor activator of NF- κ B, a member of the TNFR superfamily, *The Journal of biological chemistry* 273 (1998) 34120-34127.
- [10] L. Deng, C. Wang, E. Spencer, L. Yang, A. Braun, J. You, C. Slaughter, C. Pickart, Z. Chen, Activation of the I κ B kinase complex by TRAF6 requires a dimeric ubiquitin-conjugating enzyme complex and a unique polyubiquitin chain, *Cell* 103 (2000) 351-412.
- [11] C. Pickart, Mechanisms underlying ubiquitination, *Annual review of biochemistry* 70 (2001) 503-536.
- [12] H. Ye, J. Arron, B. Lamothe, M. Cirilli, T. Kobayashi, N. Shevde, D. Segal, O. Dzivenu, M. Vologodskaya, M. Yim, K. Du, S. Singh, J. Pike, B. Darnay, Y.

- Choi, H. Wu, Distinct molecular mechanism for initiating TRAF6 signalling, Nature 418 (2002) 443-450.
- [13] A. Kanayama, R. Seth, L. Sun, C.-K. Ea, M. Hong, A. Shaito, Y.-H. Chiu, L. Deng, Z. Chen, TAB2 and TAB3 activate the NF-kappaB pathway through binding to polyubiquitin chains, Molecular cell 15 (2004) 535-583.
- [14] C. Wang, L. Deng, M. Hong, G. Akkaraju, J. Inoue, Z. Chen, TAK1 is a ubiquitin-dependent kinase of MKK and IKK, Nature 412 (2001) 346-397
- [15] X. Feng, Regulatory roles and molecular signaling of TNF family members in osteoclasts, Gene 350 (2005) 1-14
- [16] M. Gowen, F. Lazner, R. Dodds. Cathepsin K knockout mice develop osteopetrosis due to a deficit in matrix degradation but not demineralization, Journal of Bone and Mineral Research (1999).
- [17] G. Franzoso, L. Carlson, L. Xing, L. Poljak, E.W. Shores, K.D. Brown, A. Leonardi, T. Tran, B.F. Boyce, U. Siebenlist, Requirement for NF-kappa B in osteoclast and B-cell development, Genes & Development 11 (1997).
- [18] V. Iotsova, J. Caamano, J. Loy, Y. Yang, A. Lewin, R. Bravo. Osteopetrosis in mice lacking NF-kB1 and NF-kB2, Nature Medicine 3:11 (1997).
- [19] M. Lenardo, D. Baltimore, NF-kappa B: a pleiotropic mediator of inducible and tissue-specific gene control, Cell 58 (1989) 227-236.
- [20] M. Neurath, S. Pettersson, Predominant role of NF-kappa B p65 in the pathogenesis of chronic intestinal inflammation, Immunobiology 198 (1997) 91-99.
- [21] H.-S. Liu, C.-E. Pan, Q.-G. Liu, W. Yang, X.-M. Liu, Effect of NF-kappaB and p38 MAPK in activated monocytes/macrophages on pro-inflammatory

- cytokines of rats with acute pancreatitis, *World journal of gastroenterology* : WJG 9 (2003) 2513-2521.
- [22] T. Kawai, S. Akira, The role of pattern-recognition receptors in innate immunity: update on Toll-like receptors, *Nature immunology* 11 (2010) 373-457.
- [23] S. Cordle, R. Donald, M. Read, J. Hawiger, Lipopolysaccharide induces phosphorylation of MAD3 and activation of c-Rel and related NF-kappa B proteins in human monocytic THP-1 cells, *The Journal of biological chemistry* 268 (1993) 11803-11813.
- [24] M. Muroi, T. Suzuki, Role of protein kinase A in LPS-induced activation of NF-kappa B proteins of a mouse macrophage-like cell line, J774, *Cellular signalling* 5 (1993) 289-387.
- [25] C. Janeway, R. Medzhitov, Innate immune recognition, *Annual review of immunology* 20 (2002) 197-413.
- [26] T. Ulich, L. Watson, S. Yin, P. Wang, H. Thang, J. de Castillo. Characterization of LPS-induced IL-1 and TNF mRNA Expression and the LPS-, IL-1-, and TNF-induced Inflammatory Infiltrate. *American Journal of Pathology* 138: 6 (1991).
- [27] R. Medzhitov, P. Preston-Hurlburt, E. Kopp, A. Stadlen, C. Chen, S. Ghosh, C. Janeway, MyD88 is an adaptor protein in the hToll/IL-1 receptor family signaling pathways, *Molecular cell* 2 (1998) 253-261.
- [28] S. Akira, S. Uematsu, O. Takeuchi, Pathogen recognition and innate immunity, *Cell* 124 (2006) 783-1584.
- [29] T. Kawagoe, S. Sato, K. Matsushita, H. Kato, K. Matsui, Y. Kumagai, T. Saitoh, T. Kawai, O. Takeuchi, S. Akira, Sequential control of Toll-like receptor-

- dependent responses by IRAK1 and IRAK2, *Nature immunology* 9 (2008) 684-775.
- [30] V. Bhoj, Z. Chen, Ubiquitylation in innate and adaptive immunity, *Nature* 458 (2009) 430-437.
- [31] C. Dinarello, Biologic basis for interleukin-1 in disease, *Blood* 87 (1996) 2095-2242.
- [32] S. Akira, T. Taga, T. Kishimoto. Interleukin-6 in Biology and Medicine. *Advances in Immunology* 54 (1993).
- [33] K. Tracey, Tumor necrosis factor: A pleiotropic cytokine and therapeutic target, *Annual review of medicine* (1994).
- [34] G. Mabileau, D. Chappard, A. Sabokbar, Role of the A20-TRAF6 axis in lipopolysaccharide-mediated osteoclastogenesis, *The Journal of biological chemistry* 286 (2011) 3242-3251.
- [35] Y. Abu-Amer, F. Ross, J. Edwards, S. Teitelbaum, Lipopolysaccharide-stimulated osteoclastogenesis is mediated by tumor necrosis factor via its P55 receptor, *The Journal of clinical investigation* 100 (1997) 1557-1622.
- [36] H. Zhang, H. Nguyen-Jackson, A. Panopoulos, H. Li, P. Murray, S. Watowich, STAT3 controls myeloid progenitor growth during emergency granulopoiesis, *Blood* 116 (2010) 2462-2533.
- [37] H. Qin, W.-I. Yeh, P. De Sarno, A. Holdbrooks, Y. Liu, M. Muldowney, S. Reynolds, L. Yanagisawa, T. Fox, K. Park, L. Harrington, C. Raman, E. Benveniste, Signal transducer and activator of transcription-3/suppressor of cytokine signaling-3 (STAT3/SOCS3) axis in myeloid cells regulates neuroinflammation, *Proceedings of the National Academy of Sciences of the United States of America* 109 (2012) 5004-5013.

- [38] K. El Kasmi, A. Smith, L. Williams, G. Neale, A. Panopoulos, A. Panopolous, S. Watowich, H. Hacker, B. Foxwell, P. Murray, Cutting edge: A transcriptional repressor and corepressor induced by the STAT3-regulated anti-inflammatory signaling pathway, *Journal of immunology (Baltimore, Md. : 1950)* 179 (2007) 7215-7224.
- [39] T. Smithgall, S. Briggs, S. Schreiner, E. Lerner, H. Cheng, M. Wilson, Control of myeloid differentiation and survival by Stats, *Oncogene* 19 (2000) 2612-2620.
- [40] D. Wooten, X. Xie, D. Bartos, R. Busche, G. Longmore, S. Watowich, Cytokine signaling through Stat3 activates integrins, promotes adhesion, and induces growth arrest in the myeloid cell line 32D, *The Journal of biological chemistry* 275 (2000) 26566-26641.
- [41] A. Panopoulos, L. Zhang, J. Snow, D. Jones, A. Smith, K. El Kasmi, F. Liu, M. Goldsmith, D. Link, P. Murray, S. Watowich, STAT3 governs distinct pathways in emergency granulopoiesis and mature neutrophils, *Blood* 108 (2006) 3682-3772.
- [42] H. Nguyen-Jackson, A. Panopoulos, H. Zhang, H. Li, S. Watowich, STAT3 controls the neutrophil migratory response to CXCR2 ligands by direct activation of G-CSF-induced CXCR2 expression and via modulation of CXCR2 signal transduction, *Blood* 115 (2010) 3354-3417.
- [43] T. Welte, S. Zhang, T. Wang, Z. Zhang, D. Hesslein, Z. Yin, A. Kano, Y. Iwamoto, E. Li, J. Craft, A. Bothwell, E. Fikrig, P. Koni, R. Flavell, X.-Y. Fu, STAT3 deletion during hematopoiesis causes Crohn's disease-like pathogenesis and lethality: a critical role of STAT3 in innate immunity,

Proceedings of the National Academy of Sciences of the United States of America 100 (2003) 1879-1963.

- [44] D. Aaronson, C. Horvath, A road map for those who don't know JAK-STAT, Science (New York, N.Y.) 296 (2002) 1653-1658.
- [45] D. Levy, J. Darnell, Stats: transcriptional control and biological impact, Nature reviews. Molecular cell biology 3 (2002) 651-713.
- [46] C. Luttkicken, U. Wegenka, J. Yuan, J. Buschmann, C. Schindler, A. Ziemiecki, A. Harpur, A. Wilks, K. Yasukawa, T. Taga. Association of transcription factor APRF and protein kinase JAK1 with the Interleukin-6 signal transducer gp130. Science 263 (1994).
- [47] N. Stahl, T. Boulton, T. Farruggella, N. Ip, S. Davis, B. Witthuhn, F. Quelle, O. Silvennoinen, G. Barbieri, S. Pellegrini. Association and activation of Jak-Tyk kinases by CNTF-LIF-OSM-IL-6 beta receptor components. Science 263 (1994).
- [48] S. Akira, Y. Nishio, M. Inoue, X. Wang, S. Wei, T. Matsusaka, K. Yoshida, T. Sudo, M. Naruto, T. Kishimoto. Molecular cloning of APRF, a novel IFN-stimulated Gene factor 3 p91-Related Transcription Factor Involved in the gp130-mediated signaling pathway. Cell 77 (1994).
- [49] Z. Zhong, Z. Wen, J. Darnell. Stat3: a STAT family member activated by tyrosine phosphorylation in response to epidermal growth factor and interleukin-6. Science 264 (1994).
- [50] W. Li, Canonical and non-canonical JAK-STAT signaling, Trends in cell biology 18 (2008) 545-596.
- [51] S. Akira, Functional roles of STAT family proteins: lessons from knockout mice, Stem Cells (1999).

- [52] K. Takeda, K. Noguchi, W. Shi, Targeted disruption of the mouse Stat3 gene leads to early embryonic lethality, *Proceedings of the Academy of Science* (1997).
- [53] D.E. Levy, What does Stat3 do?, *Journal of Clinical Investigation* 109 (2002).
- [54] C. Horvath, Z. Wen, J. Darnell, A STAT protein domain that determines DNA sequence recognition suggests a novel DNA-binding domain, *Genes & development* 9 (1995) 984-1078.
- [55] Z. Wen, Z. Zhong, J. Darnell, Maximal activation of transcription by Stat1 and Stat3 requires both tyrosine and serine phosphorylation, *Cell* 82 (1995) 241-291.
- [56] Z. Wen, J. Darnell, Mapping of Stat3 serine phosphorylation to a single residue (727) and evidence that serine phosphorylation has no influence on DNA binding of Stat1 and Stat3, *Nucleic acids research* 25 (1997) 2062-2069.
- [57] M. Hibi, M. Murakami, M. Saito, T. Hirano, T. Taga, T. Kishimoto. Molecular cloning and expression of an IL-6 signal transducer, gp130. *Cell* 63 (1990).
- [58] P. Heinrich, I. Behrmann, G. Muller-Newen, F. Schaper, L. Graeve, Interleukin-6-type cytokine signalling through the gp130/Jak/STAT pathway, *The Biochemical journal* 334 (Pt 2) (1998) 297-611.
- [59] H. Yu, M. Kortylewski, D. Pardoll, Crosstalk between cancer and immune cells: role of STAT3 in the tumour microenvironment, *Nature reviews. Immunology* 7 (2007) 41-92.
- [60] H. Yu, D. Pardoll, R. Jove, STATs in cancer inflammation and immunity: a leading role for STAT3, *Nature reviews. Cancer* 9 (2009) 798-1607.

- [61] S. Shi, K. Larson, D. Guo, S. Lim, P. Dutta, S.-J. Yan, W. Li, *Drosophila* STAT is required for directly maintaining HP1 localization and heterochromatin stability, *Nature cell biology* 10 (2008) 489-585.
- [62] J. Wegrzyn, R. Potla, Y.-J. Chwae, N. Sepuri, Q. Zhang, T. Koeck, M. Derecka, K. Szczepanek, M. Szelag, A. Gornicka, A. Moh, S. Moghaddas, Q. Chen, S. Bobbili, J. Cichy, J. Dulak, D. Baker, A. Wolfman, D. Stuehr, M. Hassan, X.-Y. Fu, N. Avadhani, J. Drake, P. Fawcett, E. Lesnfsky, A. Larner, Function of mitochondrial Stat3 in cellular respiration, *Science* (New York, N.Y.) 323 (2009) 793-800.
- [63] J. Yang, M. Chatterjee-Kishore, S. Staugaitis, H. Nguyen, K. Schlessinger, D. Levy, G. Stark, Novel roles of unphosphorylated STAT3 in oncogenesis and transcriptional regulation, *Cancer research* 65 (2005) 939-986.
- [64] L. Wei, G. Vahedi, H.-W. Sun, W. Watford, H. Takatori, H. Ramos, H. Takahashi, J. Liang, G. Gutierrez-Cruz, C. Zang, W. Peng, J. O'Shea, Y. Kanno, Discrete roles of STAT4 and STAT6 transcription factors in tuning epigenetic modifications and transcription during T helper cell differentiation, *Immunity* 32 (2010) 840-891.
- [65] M. Dawson, A. Bannister, B. Gottgens, S. Foster, T. Bartke, A. Green, T. Kouzarides, JAK2 phosphorylates histone H3Y41 and excludes HP1alpha from chromatin, *Nature* 461 (2009) 819-841.
- [66] Z. Zhang, T. Welte, N. Troiano, S. Maher, X.-Y. Fu, A. Bothwell, Osteoporosis with increased osteoclastogenesis in hematopoietic cell-specific STAT3-deficient mice, *Biochemical and biophysical research communications* 328 (2005) 800-807.

- [67] K. Takeda, B. Clausen, T. Kaisho, T. Tsujimura, N. Terada, I. Forster, S. Akira, Enhanced Th1 activity and development of chronic enterocolitis in mice devoid of Stat3 in macrophages and neutrophils, *Immunity* 10 (1999) 39-88.
- [68] X. Yang, A. Panopoulos, R. Nurieva, S. Chang, D. Wang, S. Watowich, C. Dong, STAT3 regulates cytokine-mediated generation of inflammatory helper T cells, *The Journal of biological chemistry* 282 (2007) 9358-9421
- [69] E. Benkhart, M. Siedlar, A. Wedel, T. Werner, H. Ziegler-Heitbrock Role of Stat3 in lipopolysaccharide-induced IL-10 gene expression, *The Journal of Immunology* (2000).
- [70] L. Williams, L. Bradley, A. Smith, B. Foxwell, Signal transducer and activator of transcription 3 is the dominant mediator of the anti-inflammatory effects of IL-10 in human macrophages, *Journal of immunology* (Baltimore, Md. : 1950) 172 (2004) 567-643.
- [71] A. O'Farrell, Y. Liu, K. Moore, A. Mui, IL-10 inhibits macrophage activation and proliferation by distinct signaling mechanisms: evidence for Stat3-dependent and -independent pathways, *The EMBO journal* 17 (1998) 1006-1024.
- [72] B. Croker, D. Krebs, J.-G. Zhang, S. Wormald, T. Willson, E. Stanley, L. Robb, C. Greenhalgh, I. Forster, B. Clausen, N. Nicola, D. Metcalf, D. Hilton, A. Roberts, W. Alexander, SOCS3 negatively regulates IL-6 signaling in vivo, *Nature immunology* 4 (2003) 540-545.
- [73] S. Grivennikov, F. Greten, M. Karin, Immunity, inflammation, and cancer, *Cell* 140 (2010) 883-982.
- [74] S. Grivennikov, M. Karin, Inflammation and oncogenesis: a vicious connection, *Current opinion in genetics & development* 20 (2010) 65-136.

- [75] A. Mantovani. Molecular Pathways linking inflammation and cancer. *Current Molecular Medicine* 10 (2010).
- [76] J. Trevino, M. Gray, S. Nawrocki, J. Summy, D. Lesslie, D. Evans, T. Sawyer, W. Shakespeare, S. Watowich, P. Chiao, D. McConkey, G. Gallick, Src activation of Stat3 is an independent requirement from NF-kappaB activation for constitutive IL-8 expression in human pancreatic adenocarcinoma cells, *Angiogenesis* 9 (2006) 101-111.
- [77] T. Bowman, M. Broome, D. Sinibaldi, W. Wharton, W. Pledger, J. Sedivy, R. Irby, T. Yeatman, S. Courtneidge, R. Jove, Stat3-mediated Myc expression is required for Src transformation and PDGF-induced mitogenesis, *Proceedings of the National Academy of Sciences of the United States of America* 98 (2001) 7319-7343.
- [78] S. Maeda, H. Kamata, J.-L. Luo, H. Leffert, M. Karin, IKKbeta couples hepatocyte death to cytokine-driven compensatory proliferation that promotes chemical hepatocarcinogenesis, *Cell* 121 (2005) 977-1067.
- [79] S. Grivennikov, E. Karin, J. Terzic, D. Mucida, G.-Y. Yu, S. Vallabhapurapu, J.r. Scheller, S. Rose-John, H. Cheroutre, L. Eckmann, M. Karin, IL-6 and Stat3 are required for survival of intestinal epithelial cells and development of colitis-associated cancer, *Cancer cell* 15 (2009) 103-116.
- [80] J. Bollrath, T. Phesse, V. von Burstin, T. Putoczki, M. Bennecke, T. Bateman, T. Nebelsiek, T. Lundgren-May, O. Canli, S. Schwitalla, V. Matthews, R. Schmid, T. Kirchner, M. Arkan, M. Ernst, F. Greten, gp130-mediated Stat3 activation in enterocytes regulates cell survival and cell-cycle progression during colitis-associated tumorigenesis, *Cancer cell* 15 (2009) 91-193.

- [81] N. Li, S. Grivennikov, M. Karin, The unholy trinity: inflammation, cytokines, and STAT3 shape the cancer microenvironment, *Cancer cell* 19 (2011) 429-460.
- [82] J. Yang, X. Liao, M. Agarwal, L. Barnes, P. Auron, G. Stark, Unphosphorylated STAT3 accumulates in response to IL-6 and activates transcription by binding to NFkappaB, *Genes & development* 21 (2007) 1396-1804.
- [83] S. Grivennikov, M. Karin, Dangerous liaisons: STAT3 and NF-kappaB collaboration and crosstalk in cancer, *Cytokine & growth factor reviews* 21 (2010) 11-20.
- [84] J. Heimall, A. Freeman, S. Holland, Pathogenesis of hyper IgE syndrome, *Clinical reviews in allergy & immunology* 38 (2010) 32-40.
- [85] I. Onal, M. Kurt, K. Altundag, S. Aksoy, M. Dincer, I. Gullu, Peripheral T-cell lymphoma and Job's syndrome: a rare association, *Medical oncology (Northwood, London, England)* 23 (2006) 141-145.
- [86] G. Leonard, E. Posadas, P. Herrmann, V. Anderson, E. Jaffe, S. Holland, W. Wilson, Non-Hodgkin's lymphoma in Job's syndrome: a case report and literature review, *Leukemia & lymphoma* 45 (2004) 2521-2526.
- [87] I. Oztop, B. Demirkan, O. Tarhan, H. Kayahan, U. Yilmaz, A. Kargi, M. Alakavuklar, The development of pulmonary adenocarcinoma in a patient with Job's syndrome, a rare immunodeficiency condition, *Tumori* 90 (2004) 132-137.
- [88] Y. Minegishi, M. Saito, S. Tsuchiya, I. Tsuge, H. Takada, T. Hara, N. Kawamura, T. Ariga, S. Pasic, O. Stojkovic, A. Metin, H. Karasuyama, Dominant-negative mutations in the DNA-binding domain of STAT3 cause hyper-IgE syndrome, *Nature* 448 (2007) 1058-1120.

- [89] S. Holland, F. DeLeo, H. Elloumi, A. Hsu, G. Uzel, N. Brodsky, A. Freeman, A. Demidowich, J. Davis, M. Turner, V. Anderson, D. Darnell, P. Welch, D. Kuhns, D. Frucht, H. Malech, J. Gallin, S. Kobayashi, A. Whitney, J. Voyich, J. Musser, C. Woellner, A. Schaffer, J. Puck, B. Grimbacher, STAT3 mutations in the hyper-IgE syndrome, *The New England journal of medicine* 357 (2007) 1608-1627.
- [90] K. Sowerwine, S. Holland, A. Freeman, Hyper-IgE syndrome update, *Annals of the New York Academy of Sciences* 1250 (2012) 25-57.
- [91] A. Freeman, D. Kleiner, H. Nadiminti, J. Davis, M. Quezado, V. Anderson, J. Puck, S. Holland, Causes of death in hyper-IgE syndrome, *The Journal of allergy and clinical immunology* 119 (2007) 1234-1274.
- [92] C. Ma, G. Chew, N. Simpson, A. Priyadarshi, M. Wong, B. Grimbacher, D. Fulcher, S. Tangye, M. Cook, Deficiency of Th17 cells in hyper IgE syndrome due to mutations in STAT3, *The Journal of experimental medicine* 205 (2008) 1551-1558.
- [93] J. Milner, J. Brenchley, A. Laurence, A. Freeman, B. Hill, K. Elias, Y. Kanno, C. Spalding, H. Elloumi, M. Paulson, J. Davis, A. Hsu, A. Asher, J. O'Shea, S. Holland, W. Paul, D. Douek, Impaired T(H)17 cell differentiation in subjects with autosomal dominant hyper-IgE syndrome, *Nature* 452 (2008) 773-779.
- [94] L. de Beaucoudrey, A. Puel, O.e. Filipe-Santos, A.I. Cobat, P. Ghandil, M. Chrabieh, J. Feinberg, H. von Bernuth, A. Samarina, L. Janniere, C. Fieschi, J.-L. Stephan, C. Boileau, S. Lyonnet, G. Jondeau, V.r. Cormier-Daire, M. Le Merrer, C. Hoarau, Y. Lebranchu, O. Lortholary, M.-O. Chandesris, F.o. Tron, E. Gambineri, L. Bianchi, C. Rodriguez-Gallego, S. Zitnik, J. Vasconcelos, M. Guedes, A. Vitor, L. Marodi, H. Chapel, B. Reid, C. Roifman, D. Nadal, J.

- Reichenbach, I. Caragol, B.-Z. Garty, F. Dogu, Y. Camcioglu, S. Gaulle, O. Sanal, A. Fischer, L. Abel, B. Stockinger, C. Picard, J.-L. Casanova, Mutations in STAT3 and IL12RB1 impair the development of human IL-17-producing T cells, *The Journal of experimental medicine* 205 (2008) 1543-1593.
- [95] M. Saito, M. Nagasawa, H. Takada, T. Hara, S. Tsuchiya, K. Agematsu, M. Yamada, N. Kawamura, T. Ariga, I. Tsuge, S. Nonoyama, H. Karasuyama, Y. Minegishi, Defective IL-10 signaling in hyper-IgE syndrome results in impaired generation of tolerogenic dendritic cells and induced regulatory T cells, *The Journal of experimental medicine* 208 (2011) 235-284.
- [96] M. Giacomelli, N. Tamassia, D. Moratto, P. Bertolini, G. Ricci, C. Bertulli, A. Plebani, M. Cassatella, F. Bazzoni, R. Badolato, SH2-domain mutations in STAT3 in hyper-IgE syndrome patients result in impairment of IL-10 function, *European journal of immunology* 41 (2011) 3075-3159.
- [97] H. Lee, A. Herrmann, J.-H. Deng, M. Kujawski, G. Niu, Z. Li, S. Forman, R. Jove, D. Pardoll, H. Yu, Persistently activated Stat3 maintains constitutive NF-kappaB activity in tumors, *Cancer cell* 15 (2009) 283-376.
- [98] E. Renner, S. Rylaarsdam, S. Anover-Sombke, A. Rack, J. Reichenbach, J. Carey, Q. Zhu, A. Jansson, J. Barboza, L. Schimke, M. Leppert, M. Getz, R. Seger, H. Hill, B. Belohradsky, T. Torgerson, H. Ochs, Novel signal transducer and activator of transcription 3 (STAT3) mutations, reduced T(H)17 cell numbers, and variably defective STAT3 phosphorylation in hyper-IgE syndrome, *The Journal of allergy and clinical immunology* 122 (2008) 181-188.
- [99] A. Yoshimura, T. Naka, M. Kubo, SOCS proteins, cytokine signalling and immune regulation, *Nature reviews. Immunology* 7 (2007) 454-519.

- [100] L. Zhang, D. Badgwell, J. Bevers, K. Schlessinger, P. Murray, D. Levy, S. Watowich, IL-6 signaling via the STAT3/SOCS3 pathway: functional analysis of the conserved STAT3 N-domain, *Molecular and cellular biochemistry* 288 (2006) 179-268.
- [101] C. Auernhammer, C. Bousquet, S. Melmed, Autoregulation of pituitary corticotroph SOCS-3 expression: characterization of the murine SOCS-3 promoter, *Proceedings of the National Academy of Sciences of the United States of America* 96 (1999) 6964-6973.
- [102] D. Krebs, D. Hilton, SOCS proteins: negative regulators of cytokine signaling, *Stem cells (Dayton, Ohio)* 19 (2001) 378-465.
- [103] W. Boyle, W. Simonet, D. Lacey, Osteoclast differentiation and activation, *Nature* 423 (2003) 337-379.
- [104] W. Liu, Functional Identification of Three Receptor Activator of NF- κ B Cytoplasmic Motifs Mediating Osteoclast Differentiation and Function, *Journal of Biological Chemistry* 279 (2004)
- [105] P. Collin-Osdoby, P. Osdoby, RANKL-mediated osteoclast formation from murine RAW 264.7 cells, *Methods in molecular biology (Clifton, N.J.)* 816 (2012) 187-389
- [106] V. Cristina, K. Masakazu, M.F. David, J.A. Gerald, The generation of osteoclasts from RAW 264.7 precursors in defined, serum-free conditions, *Journal of Bone and Mineral Metabolism* 27 (2008).
- [107] H. Ichikawa, 1'-Acetoxychavicol Acetate Inhibits RANKL-Induced Osteoclastic Differentiation of RAW 264.7 Monocytic Cells by Suppressing Nuclear Factor- κ B Activation, *Molecular Cancer Research* 4 (2006).

- [108] M. Rahman, A. Bhattacharya, G. Fernandes, Docosahexaenoic acid is more potent inhibitor of osteoclast differentiation in RAW 264.7 cells than eicosapentaenoic acid, *Journal of cellular physiology* 214 (2008) 201-210.
- [109] S. Ghisletti, W. Huang, K. Jepsen, C. Benner, G. Hardiman, M. Rosenfeld, C. Glass, Cooperative NCoR/SMRT interactions establish a corepressor-based strategy for integration of inflammatory and anti-inflammatory signaling pathways, *Genes & development* 23 (2009) 681-774.
- [110] J.-Y. Yoo, H.-K. Choi, K.-C. Choi, S.-Y. Park, I. Ota, J. Yook, Y.-H. Lee, K. Kim, H.-G. Yoon, Nuclear hormone receptor corepressor promotes esophageal cancer cell invasion by transcriptional repression of interferon-g-inducible protein 10 in a casein kinase 2-dependent manner, *Molecular biology of the cell* 23 (2012) 2943-5897.
- [111] H. Khalaf, J. Jass, P. Olsson. Differential cytokine regulation by NF- κ B and AP-1 in Jurkat T-cells, *BMC immunology* (2010).
- [112] D. Krappmann, E. Wegener, Y. Sunami, M. Esen, A. Thiel, B. Mordmuller, C. Scheidereit, The I κ B kinase complex and NF- κ B act as master regulators of lipopolysaccharide-induced gene expression and control subordinate activation of AP-1, *Molecular and cellular biology* 24 (2004) 6488-6988.
- [113] J. Wan, L. Sun, J. Mendoza, Y. Chui, D. Huang, Z. Chen, N. Suzuki, S. Suzuki, W.-C. Yeh, S. Akira, K. Matsumoto, Z.-G. Liu, Z. Wu, Elucidation of the c-Jun N-terminal kinase pathway mediated by Esten-Barr virus-encoded latent membrane protein 1, *Molecular and cellular biology* 24 (2004) 192-201.

- [114]M. Czaja, The future of GI and liver research: editorial perspectives. III.
JNK/AP-1 regulation of hepatocyte death, American journal of physiology.
Gastrointestinal and liver physiology 284 (2003) 9.
- [115]D. Sheppard, Dominant negative mutants: tools for the study of protein function
in vitro and in vivo, American journal of respiratory cell and molecular biology
11 (1994) 1-7.
- [116]A. Harris, S. Dial, D. Casciano, Comparison of basal gene expression profiles
and effects of hepatocarcinogens on gene expression in cultured primary
human hepatocytes and HepG2 cells, Mutation research 549 (2004) 79-178.
- [117]H. Jianxin, S. Jie, X. Ximing, Z. Wenhua, W. Yuxin, C. Xing, D. Yuping, Z.
Ning, Z. Jing, W. Qin, Y. Jinbo, STAT3 mutations correlated with hyper-IgE
syndrome lead to blockage of IL-6/STAT3 signalling pathway, Journal of
Biosciences 37 (2012).
- [118]G. He, M. Karin, NF-kB and STAT3 - key players in liver inflammation and
cancer, Cell research 21 (2011) 159-227.
- [119]F. Greten, L. Eckmann, T. Greten, J. Park, Z.-W. Li, L. Egan, M. Kagnoff, M.
Karin, IKKbeta links inflammation and tumorigenesis in a mouse model of
colitis-associated cancer, Cell 118 (2004) 285-381.
- [120]J. Gohda, T. Matsumura, J. Inoue. Cutting edge: TNFR-associated factor
(TRAF) 6 is essential for MyD88-dependent pathway but not Toll/IL-1 receptor
domain-containing adaptor-inducing IFN- β (TRIF)-dependent Pathway in TLR
signaling. The Journal of Immunology (2004).
- [121]B. Grimbacher, S. Holland, J. Gallin, F. Greenberg, S. Hill, H. Malech, J. Miller,
A. O'Connell, J. Puck, Hyper-IgE syndrome with recurrent infections--an

autosomal dominant multisystem disorder, The New England journal of medicine 340 (1999) 692-1394.

[122]M. Karin, Y. Ben-Neriah. Phosphorylation Meets Ubiquitination: The Control of NFkB Activity. Annual Review of Immunology 18 (2000).

Vita

Nathaniel Robert Greeley was born in Denver, Colorado on December 29, 1986. He is the child of Laura H. Carpenter and David F. Greeley. After completing high school at Strake Jesuit College Preparatory in Houston, Texas, he attended the University of Colorado at Boulder where he earned his Bachelor's of Arts in Molecular, Cellular and Developmental Biology in May 2009. In June 2009, he worked as a Research Assistant at the M.D. Anderson Cancer Center until he enrolled in the University of Texas Health Science Center at Houston's Graduate School of Biomedical Sciences in August, 2010. Nathaniel performed this Master's thesis work in the Department of Immunology under the mentorship of Dr. Stephanie Watowich, Ph.D. This work was completed August 31, 2012.